

NUSC Technical Report 5633

AD A 043359

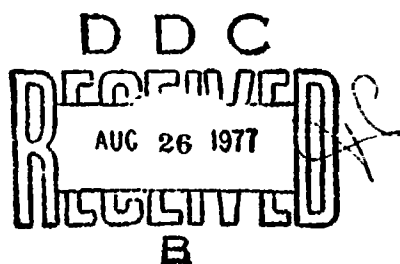
NUSC Technical Report 5633



12

Underwater Helmholtz- Resonator Transducers: General Design Principles

Ralph S. Woollett
Special Projects Department



5 July 1977

NUSC

NAVAL UNDERWATER SYSTEMS CENTER
Newport, Rhode Island • New London, Connecticut

Approved for public release, distribution unlimited.

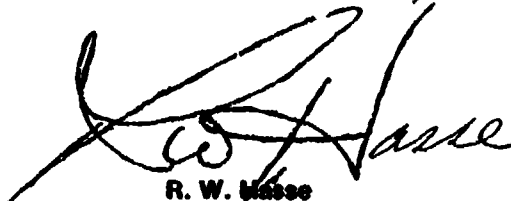
AD No. _____
DDC FILE COPY

PREFACE

This study was conducted under NUJSC Project No. A-720-01, "Transduction Techniques for Navy Sonar Transducers," Principal Investigator, C. L. LeBlanc (Code 316), and Navy Subproject and Task No. SF11 121 603, Program Manager, C. C. Walker (Code NAVSEA 06H1-2).

The Technical Reviewer for this report was L. C. Maples (Code 313).

REVIEWED AND APPROVED: 5 July 1977

A handwritten signature in black ink, appearing to read "R. W. Masse", is written over a horizontal line.

R. W. Masse
Head, Special Projects Department

The author of this report is located at the New London
Laboratory, Naval Underwater Systems Center,
New London, Connecticut 06320.

REPORT DOCUMENTATION PAGE		READ INSTRUCTIONS BEFORE COMPLETING FORM
1. REPORT NUMBER TR-5633	2. GOVT ACCESSION NO.	3. RECIPIENT'S CATALOG NUMBER
4. TITLE (and Subtitle) UNDERWATER HELMHOLTZ-RESONATOR TRANSDUCERS: GENERAL DESIGN PRINCIPLES,		5. TYPE OF REPORT & PERIOD COVERED
6. AUTHOR(S) Ralph S. Woollett		7. PERFORMING ORG. REPORT NUMBER
8. PERFORMING ORGANIZATION NAME AND ADDRESS Naval Underwater Systems Center New London Laboratory New London, CT 06320		9. CONTRACT OR GRANT NUMBER(s)
10. CONTROLLING OFFICE NAME AND ADDRESS Naval Sea Systems Command (06H1-2) Washington, DC 20362		11. PROGRAM ELEMENT, PROJECT, TASK AREA & WORK UNIT NUMBERS A72001 SF11 121 603
12. MONITORING AGENCY NAME & ADDRESS (if different from Controlling Office) (12) 46P.1		13. REPORT DATE 5 Jul 77
		14. NUMBER OF PAGES 44
		15. SECURITY CLASS. (of this report) UNCLASSIFIED
		16. DECLASSIFICATION/DOWNGRADING SCHEDULE
17. DISTRIBUTION STATEMENT (of this Report) Approved for public release; distribution unlimited. (16) F11121		
18. DISTRIBUTION STATEMENT (of the abstract entered in Block 20, if different from Report) (17) F11121 643		
19. SUPPLEMENTARY NOTES		
20. KEY WORDS (Continue on reverse side if necessary and identify by block number) Acoustical Compliant Tubes Piezoelectric Ring Stacks Acoustoelectrical Feedback Sonar Transducers Helmholtz-Resonator Transducers Very Low Frequency Sound Sources Piezoelectric Flexural Disks		
21. ABSTRACT (Continue on reverse side if necessary and identify by block number) Underwater Helmholtz resonators excited by piezoelectric drivers show promise as compact sound sources for very low frequencies. Since 1969, Groves and Henriquez of the Naval Research Laboratory have been using small spherical shells of piezoelectric ceramic as Helmholtz-resonator transducers. The object of the present study was to investigate more general configurations for Helmholtz resonators and to evolve optimum designs. Primary interest was in developing a new approach to generating sound at frequencies below 100 Hz, where existing capabilities were very limited.		

20. Cont'd

Some of the principal avenues of development were (1) application of flexural disks to drive the resonators and comparative evaluation of disk and ring drivers, (2) introduction of compliant tubes into the compliance chamber to decrease its size, and (3) application of acoustoelectrical feedback to broaden the response at resonance. The study was conducted using a lumped-parameter approach and electroacoustical circuit analysis. Experiments with small-size models confirmed the general validity of this approach.

A design procedure for disk-driven Helmholtz resonators is outlined. A numerical example illustrating the procedure indicates that a flexural disk 1-meter in diameter driving a Helmholtz resonator resonant at 40 Hz should be capable of producing a narrowband source level of 196 dB/ $1\mu\text{Pa}\cdot\text{m}$. It would also be useful as a broadband source, producing 185 dB source level over a band 37-100 Hz. The transducer would have a maximum depth capability of 450 m and a required minimum depth of 11 m to suppress internal cavitation.

TABLE OF CONTENTS

	Page
LIST OF ILLUSTRATIONS	ii
INTRODUCTION	1
OPERATING PRINCIPLES AND ANALYSIS METHODS	6
GENERAL DESIGN PRINCIPLES	9
CERAMIC DRIVER CHARACTERISTICS	17
Ring Stack	17
Trilaminar Disk	20
Comparison of Ring With Disk	21
NARROWBAND DESIGN	22
BROADBAND DESIGN	25
EFFECTS OF TRANSDUCER SIZE	27
EFFECTS OF DEPTH REQUIREMENTS	30
DESIGN PROCEDURE FOR THE DISK-DRIVEN HELMHOLTZ RESONATOR	31
STATUS OF HELMHOLTZ-RESONATOR INVESTIGATIONS	37
FUTURE WORK	39
REFERENCES	40

ACCESSION for	
NTIS	White Section <input checked="" type="checkbox"/>
DDC	Bull Section <input type="checkbox"/>
UNANNOUNCED	<input type="checkbox"/>
JUSTIFICATION	
BY	
DISTRIBUTION/AVAILABILITY CODES	
Dist.	ACRIL END/CI SPECIAL
A	

LIST OF ILLUSTRATIONS

Figure		Page
1	Three Approaches to Cavity Compliance	2
2	Helmholtz-Resonator Transducer Parts Ready for Assembly, With Compliant-Tube Pack in Foreground	4
3	Helmholtz-Resonator Transducer With Compliant-Tube Pack Installed and Trilaminar Disk Positioned for Bolting to Compliance Chamber	5
4	Transmitting Voltage Response of a Helmholtz-Resonator Transducer	6
5	Electroacoustical Circuit of the Helmholtz-Resonator Transducer	7
6	Source Level Curve of a Helmholtz Resonator, Showing Voltage and Stress Limits	11
7	Maximum Source Level Envelope. The Broadband Power P_{BB} Is Determined by the Level of the Curve at the Saddle, at a Frequency of About $1.4 f_r$	12
8	Shaping of the Source-Level Curve for Narrowband Applica- tions	14
9	Shaping of the Source-Level Curve for Broadband Applica- tions	15
10	Circuitry for Shaping the Source-Level Curve	16
11	Piezoelectric Ceramic Drivers	18
12	Double-Disk Helmholtz Resonator With Radial-Flow Ports .	22
13	Predicted Source Level and Stress Level for a 40 Hz Helmholtz-Resonator Transducer Driven by a 1-m Disk	36
14	Measured and Calculated Source Levels for an Experimental Model	38

UNDERWATER HELMHOLTZ-RESONATOR TRANSDUCERS: GENERAL DESIGN PRINCIPLES

INTRODUCTION

In 1972 a study began that was directed at establishing the capabilities of underwater sound sources based on the Helmholtz-resonator configuration. The primary interest was in developing a new approach to generating sound at frequencies below 100 Hz, where existing capabilities were very limited. In this report the general principles governing the design of Helmholtz-resonator transducers will be presented. Design equations will be introduced as needed, but in order to keep attention focused on the physical aspects of design, the detailed derivation of the equations will not be included. This area will be covered in a subsequent report. Similarly, only a brief summary of the experimental results will be included. A measurement program on small-size Helmholtz-resonator transducers has been underway for two years, and a number of publications will be needed to present the results obtained on the different models.

The Helmholtz resonators in this study are excited by piezoelectric ceramic drivers. The Helmholtz resonator introduces a resonance much lower in frequency than that of the ceramic driver by itself and hence extends the useful range of piezoceramic transducers to lower frequencies. Although interest is primarily in the frequency range below 100 Hz, the techniques explored here might be found useful at frequencies up to 1000 Hz, or more, when compact transducers are desired.

The ceramic driver can be in the form of a spherical shell, a stack of ceramic rings, or a flexural-mode disk. The cavity of the Helmholtz resonator can be filled with liquid only, liquid plus compliant tubes, or compressed gas. Figure 1 shows transducers with these three types of compliance cavities. A flexural-disk driver is used in each case for illustrative purposes. The transducer with purely liquid fill has unlimited depth capability. The transducer with compliant tubes is suitable for operation to depths of about 600 meters; its depth limitation is determined by the strength of the compliant tubes. The transducer with compressed gas is limited to operation at a relatively fixed depth since its resonance frequency varies with depth. The interior compressibility of the three models in figure 1 increases from one model to the next in descending order in the figure. High compressibility is desirable because it leads to small cavity size and, therefore, low transducer weight. Most of the attention in this report will be devoted to designs using compliant tubes.

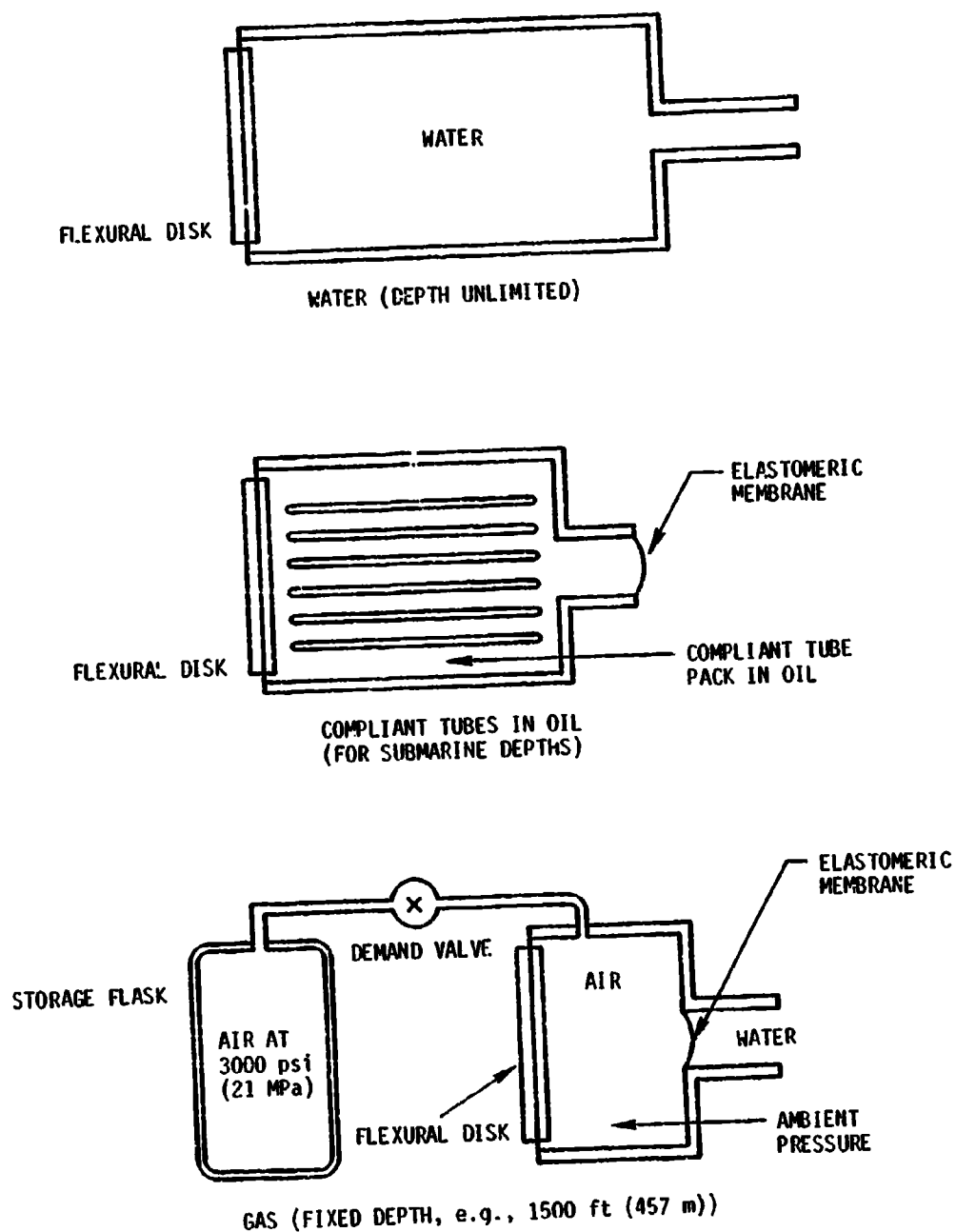


Figure 1. Three Approaches to Cavity Compliance

When a stack of ceramic rings is used as the driver, the rings form the cylindrical wall of the cavity. The flexural disk shown in figure 1 would then be replaced by a rigid metal plate. If a spherical ceramic shell were used it would form the entire cavity. Spherical shells perform very similarly to ring stacks. They were not considered explicitly in the designs in this report because they are difficult to make in the large sizes contemplated.

Figures 2 and 3 show an experimental model of a Helmholtz-resonator transducer. A number of similar models were constructed with different cavity lengths and different necks. The interior diameter of these transducers is 16.5 cm, and the resonance frequencies of the different models lie in the range of 130 to 700 Hz. This frequency range was chosen so that the models would be economically small, but the purpose of the experiments was to provide information that could be used in designing lower-frequency transducers. Plastic compliant tubes were used in these models, but metal compliant tubes would be used in the full-scale transducers, since the metal tubes are superior in this application.¹

Figure 4 shows the form of the transmitting voltage response of the Helmholtz-resonator transducer. The high-frequency resonance is that of the ceramic driver, and it is not of interest for narrowband applications but it may contribute to the passband in very broadband applications. The low-frequency resonance is the Helmholtz resonance, which is the main concern of this study. The response in between the two resonances has a slope of 12 dB/octave.

The history of underwater Helmholtz resonators in sonar began with ceramic hydrophones that were liquid-filled and had a small opening to equalize the internal and external pressures. Such a device constituted a Helmholtz resonator, with the resonance located at the lower end of the hydrophone's receiving band. The Helmholtz resonance was a side effect as far as the designer was concerned, and usually he made the damping in the neck (or orifice) so high that the resonance was overdamped. Later, advantage was taken of the Helmholtz resonance to enhance the low-frequency response of a reciprocal transducer,² and finally a spherical-shell transducer was designed specifically as a Helmholtz-resonator sound source.³

The present study was undertaken with the aim of developing design principles to the point where Helmholtz-resonator transducers could be fully exploited. Some of the principal avenues of development were the following:

1. Application of flexural disks to drive the resonator, and comparative evaluation of disk and ring drivers;
2. Introduction of compliant tubes to decrease the size of the compliance chamber; and

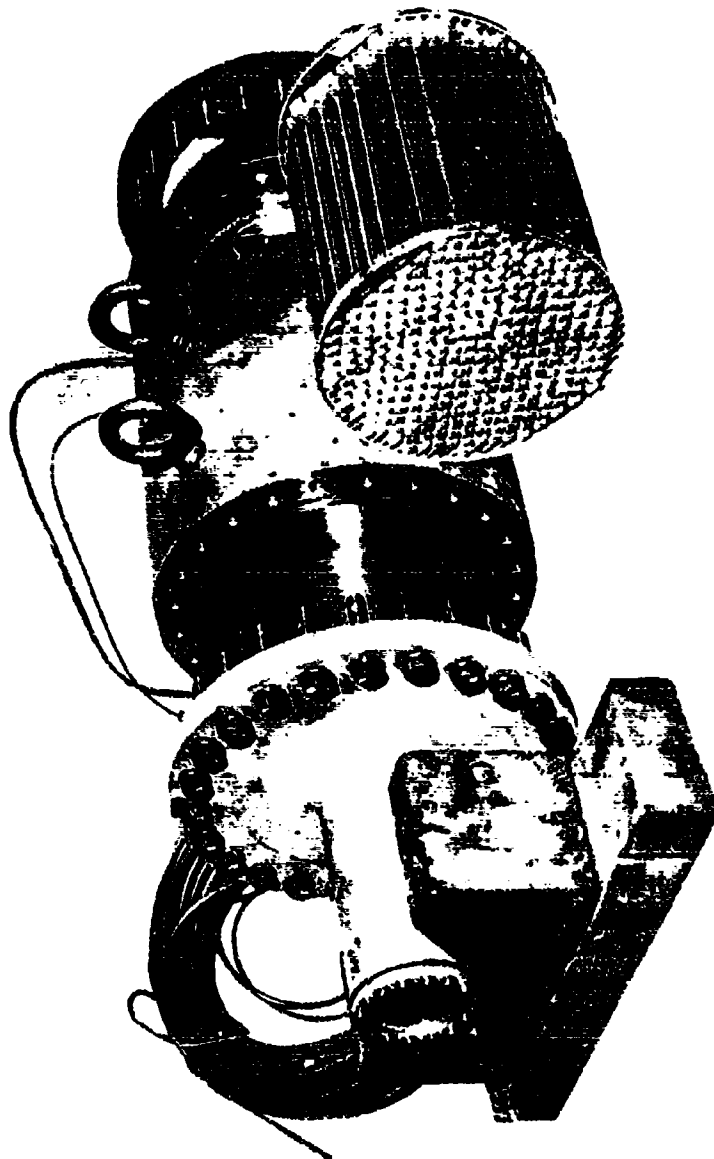


Figure 2. Helmholtz-Resonator Transducer Parts Ready for Assembly, With Compliant-Tube Pack in Foreground

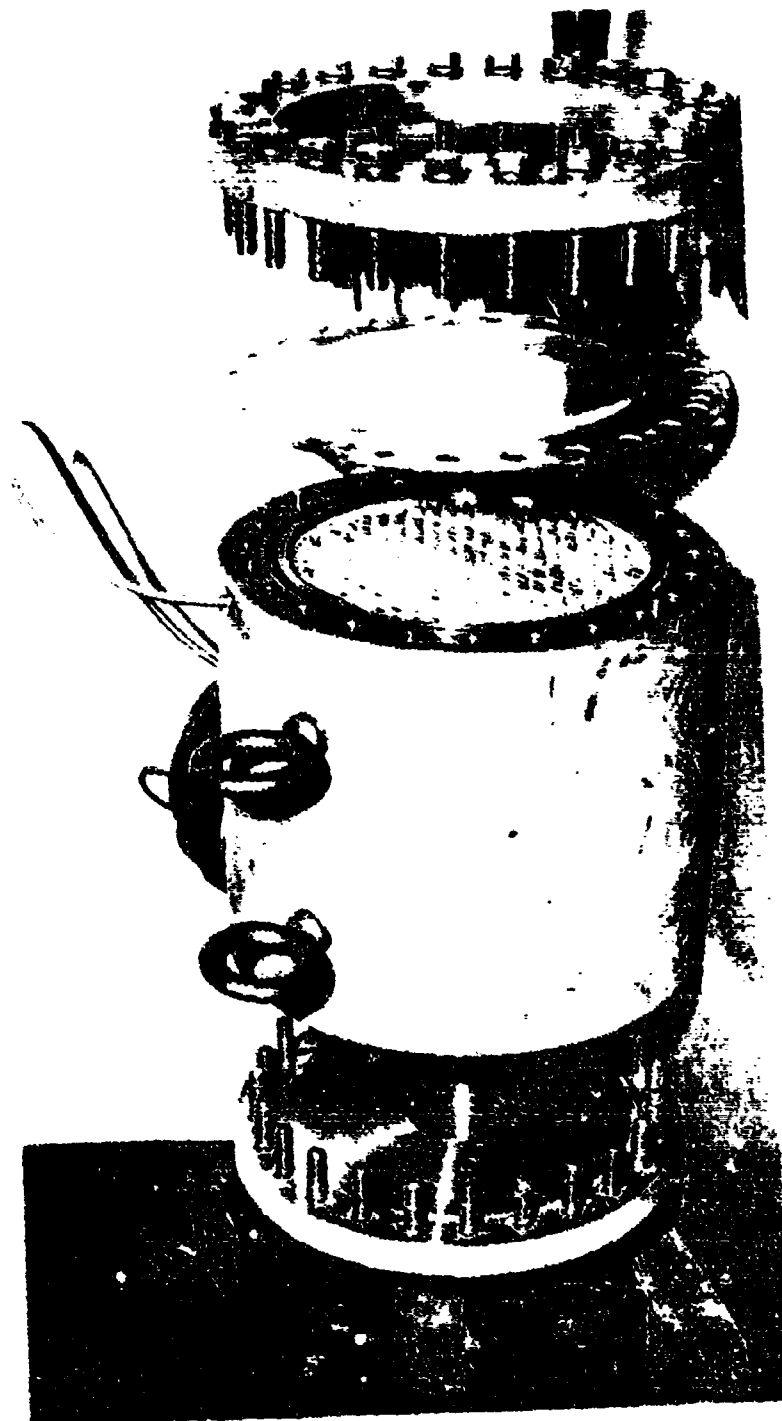


Figure 3. Helmholtz-Resonator Transducer With Compliant-Tube Pack
Installed and Trilaminar Disk Positioned for Bolting to Compliance Chamber

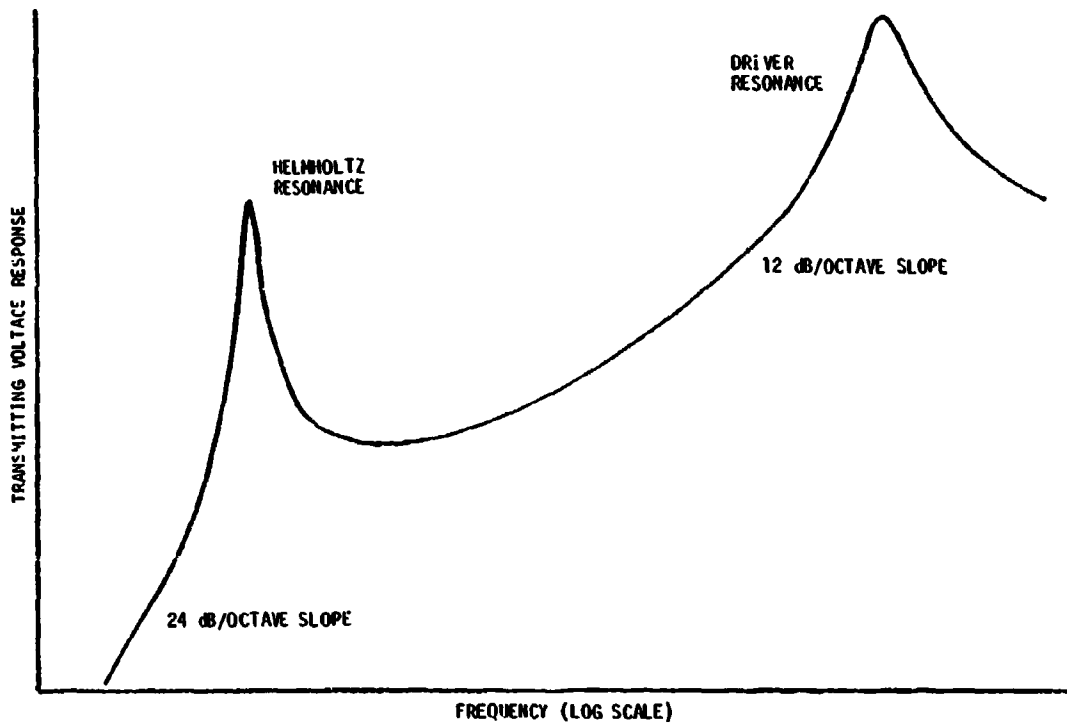


Figure 4. Transmitting Voltage Response of a Helmholtz-Resonator Transducer

3. Application of acoustoelectric feedback to broaden the response at resonance.

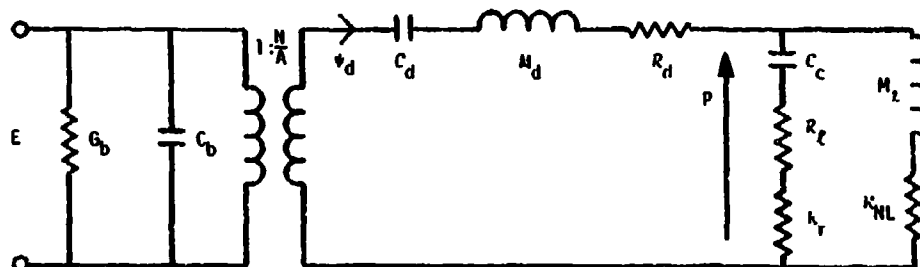
The evolution of some of these ideas is described in earlier publications.^{4,5,6}

OPERATING PRINCIPLES AND ANALYSIS METHODS

The ceramic driver of the Helmholtz resonator radiates directly into the external medium as well as into the cavity. Energy radiated into the cavity emerges from the neck and interacts with that radiated by the outside surface of the driver. If the designer should wish to use only the neck radiation, he would have to provide acoustic isolation (incorporating pressure-release materials) on the outside surface of the driver. This complication would destroy the attractive features of the Helmholtz resonator. However, avoidance of the acoustic interaction

is not necessarily a desideratum; the interaction is destructive only below resonance. At resonance the two radiations are in phase quadrature, and the neck radiation predominates. Above resonance the two radiations are in phase, and the neck radiation falls off rapidly with increasing frequency. In this region the response essentially is that which the driver would have if it were used in the conventional way with a pressure-release interior.

A lumped-parameter approach is adequate for describing the Helmholtz-resonator transducer in the typical configurations considered here. The electroacoustical circuit diagram of the transducer is shown in figure 5. The design equations, and all conclusions about performance, are based on analysis of this circuit. The portion of the circuit on the left of the electroacoustical transformer is electrical; the portion on the right is acoustical. In the acoustical portion, the variables are pressure, P , which is analogous to voltage, and volume velocity, ψ , which is analogous to current. The equations that will be included in this report for circuit parameters, or for transducer characteristics, are based on the use of SI units.



- C_b = BLOCKED CAPACITY
- G_b = LOSS CONDUCTANCE OF CERAMIC
- N = ELECTROMECHANICAL RATIO OF CERAMIC DRIVER
- A = AREA (ONE SIDE) OF CERAMIC DRIVER
- E = DRIVING VOLTAGE
- ψ_d = VOLUME VELOCITY OF DRIVER
- P = AC PRESSURE IN THE CAVITY
- C_d = ACOUSTIC COMPLIANCE OF DRIVER
- M_d = ACOUSTIC INERTANCE OF DRIVER
- R_d = ACOUSTIC RESISTANCE OF DRIVER
- C_c = ACOUSTIC COMPLIANCE OF CAVITY
- M_c = ACOUSTIC INERTANCE OF NECK OR ORIFICE
- R_c = ACOUSTIC RESISTANCE (VISCOUS) OF CAVITY
- R_r = ACOUSTIC RADIATION RESISTANCE
- R_{NL} = NONLINEAR ORIFICE RESISTANCE

Figure 5. Electroacoustical Circuit of the Helmholtz-Resonator Transducer

In the circuit, the output power is the power dissipated in the radiation resistance R_r . Radiation is due to the net-volume velocity ($\psi_m - \psi_d$) of the transducer, and in the circuit this net-volume velocity flows through the branch containing C_c ; hence, the radiation resistance belongs in this branch.⁷ Mutual radiation resistance between the neck and the outside of the driver is then automatically taken care of. The equation for the acoustical radiation resistance is remarkably simple:

$$R_r = 2.16f^2, \quad (1)$$

where f is the frequency.

When the transducers are compact (very small compared with the wavelength), R_r will be small compared with the loss resistance R_l and the reactance $1/\omega C_c$. Then the Q of the Helmholtz resonance will be controlled by the losses and will be very high when the losses are carefully minimized.

The pressure, P , is the ac pressure in the cavity, and it peaks at the resonance frequency. The internal pressure is higher than the near-field external pressure; so when cavitation occurs because of inadequate depth, it will occur internally. Even in the absence of cavitation, the buildup of cavity pressure at resonance must be kept under control because it can go high enough to fracture the ceramic driver. The operating resonance frequency depends on C_d as well as C_c and is given by the equation

$$f_r = \frac{1}{2\pi} \sqrt{\frac{1}{(C_d + C_c)M_l}} \quad (2)$$

In describing the ceramic driver, two properties that are indicative of its capability are the free-volume displacement, ΔV_f , and the blocked pressure, P_b . The relation between the two is given by the equation

$$\Delta V_f = P_b C_d = \frac{N}{A} E C_d. \quad (3)$$

The properties of the flexural-disk driver are given with sufficient accuracy for initial design studies by available approximate formulas.⁸ The final disk parameters may be obtained with refined accuracy from an existing computer program.^{9,10,11}

The loss resistances, R_l and R_d , cannot be calculated from theory, and one of the principal aims of the experimental program was to obtain information on them. The neck inertance, M_l , can be calculated with fair accuracy, but an interior-end correction is involved that is uncertain for these designs; so this subject is being investigated experimentally. At high-driving levels a nonlinear-loss resistance will appear in series with M_l on the circuit diagram. Formulas for this resistance are only

approximate; so, again, improved information on this effect is being sought from the experiments.

In the region of the Helmholtz resonance, the ceramic driver is stiffness controlled, and its inertance, M_d , and resistance, R_d , may be neglected. This assumption is incorporated in the equations of this report. When performance data well above resonance are required, M_d and R_d must be included in the circuit. Then the circuit computations are carried out on the HP-9820 calculator. This calculator is very well suited to this problem and will plot very rapidly any response curves that may be desired.

GENERAL DESIGN PRINCIPLES

Given a set of performance goals, the designer's task is centered around choosing the optimum ceramic driver and the optimum compliance cavity for the Helmholtz resonator.

The ceramic driver operates well below its self-resonance when driving the Helmholtz resonance, and its internal impedance reduces simply to its quasi-static compliance, C_d . The driver is judged primarily by the power capability it imparts to the Helmholtz source. The chief property which determines this is the volume displacement, ΔV_f , that the driver is able to produce in an adjoining medium in the absence of any back pressure. To maximize this free-volume displacement, one of course operates the ceramic at maximum-allowable electric-field intensity, which in this study is taken to be 4 kV/cm rms.

Another property of the driver that influences power capability (but only in the resonance region) is P_{max} , the maximum pressure that the driver can withstand safely without fracturing. This pressure is related through geometrical factors to the fracture stress of the ceramic, T_{max} , which in this study is taken to be 14 MPa (2000 psi).

The compliance chamber is characterized by its acoustic compliance, C_c , and its viscous loss resistance, R_c . The compliance, C_c , increases as the chamber volume is increased and as the packing of the chamber with compliant tubes is increased. It also depends on the elastic properties of the compliant tubes, on the stiffness of the chamber walls, and on the compressibility of the enclosed liquid. The loss resistance, R_c , decreases as the volume of the chamber is increased, but increases as the tube-packing factor is increased. It depends also on the kinematic viscosity of the enclosed liquid.

The relation of the cavity compliance, C_c , to the driver compliance, C_d , is an important consideration in design; so a parameter, α , that

specifies this relation is introduced:

$$\alpha = \frac{C_d}{C_d + C_c} < 1 \quad (4)$$

In the designs under consideration, α is considerably less than 1. Thus the net compliance of the resonator is mainly that of the cavity.

The compliance cavity constitutes the biggest (and heaviest) section of the resonator structure. Hence, one is motivated to try to reduce its size (thereby reducing C_c). Such a reduction has the following effects:

1. Raises cavity pressure, P , at resonance;
2. Increases the loss resistance;
3. Increases neck length (to maintain resonance); and
4. Increases α .

For the most part these effects are undesirable, although increasing α increases the electroacoustical coupling factor, which is beneficial. Balancing these effects against the benefits of size reduction will constitute a considerable part of the design process. The procedure will be illustrated in the following sections of this report.

The maximum source-level curve of the Helmholtz-resonator transducer is illustrated in figure 6. Away from resonance, the source level is limited by the maximum-allowable voltage, which for a given driver determines the achievable volume displacement, ΔV_f . The equation for the power output is

$$P = 42.6 f^4 (1 - \alpha)^2 \left[\frac{\Delta V_f}{\left(\frac{f_r}{f} \right)^2 - 1} \right]^2, \quad f \neq f_r \quad (5)$$

Normally, $\alpha < 0.3$; then the off-resonance source level is determined within 3 dB as soon as the driver is chosen, since ΔV_f is a property of the driver. Thus, the off-resonance source level is essentially established before the compliance C_c is chosen.

When the frequency is swept through resonance, the ac pressure in the cavity rises, and if maximum voltage is maintained the ceramic is liable to fracture as a result of excessive pressure. Therefore, the voltage may have to be reduced in the resonance region, with a

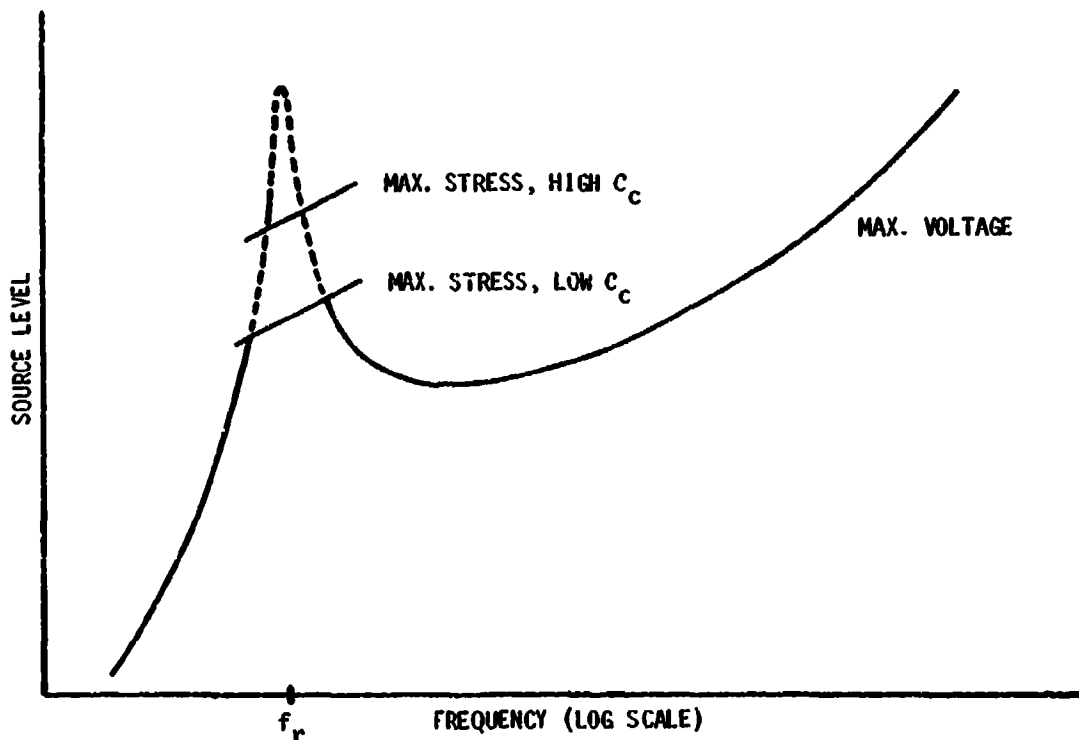


Figure 6. Source Level Curve of a Helmholtz Resonator, Showing Voltage and Stress Limits

corresponding reduction in source level. This source-level limit, determined by ceramic fracture, is indicated in figure 6, and is labeled maximum stress. The equation for the stress limit lines is

$$P_{\max} = 42.6 f^4 C_c^2 p_{\max}^2 \quad (6)$$

The stress-limited power depends not only on the pressure limit, P_{\max} , of the driver, but also on the cavity compliance, C_c . Choice of C_c will therefore depend, among other things, on how high a source-level rise around resonance is desired. The height of the stress-limit line relative to the voltage-limit curve above resonance, when expressed in decibels, is $20 \log [(1/\alpha)(P_{\max}/P_b)]$ (figure 7). In this expression, P_{\max}/P_b is the ratio of fracture pressure to the maximum electrically generated pressure, and is of the order of unity. The blocked pressure, P_b , is related to ΔV_f as indicated in equation (3).

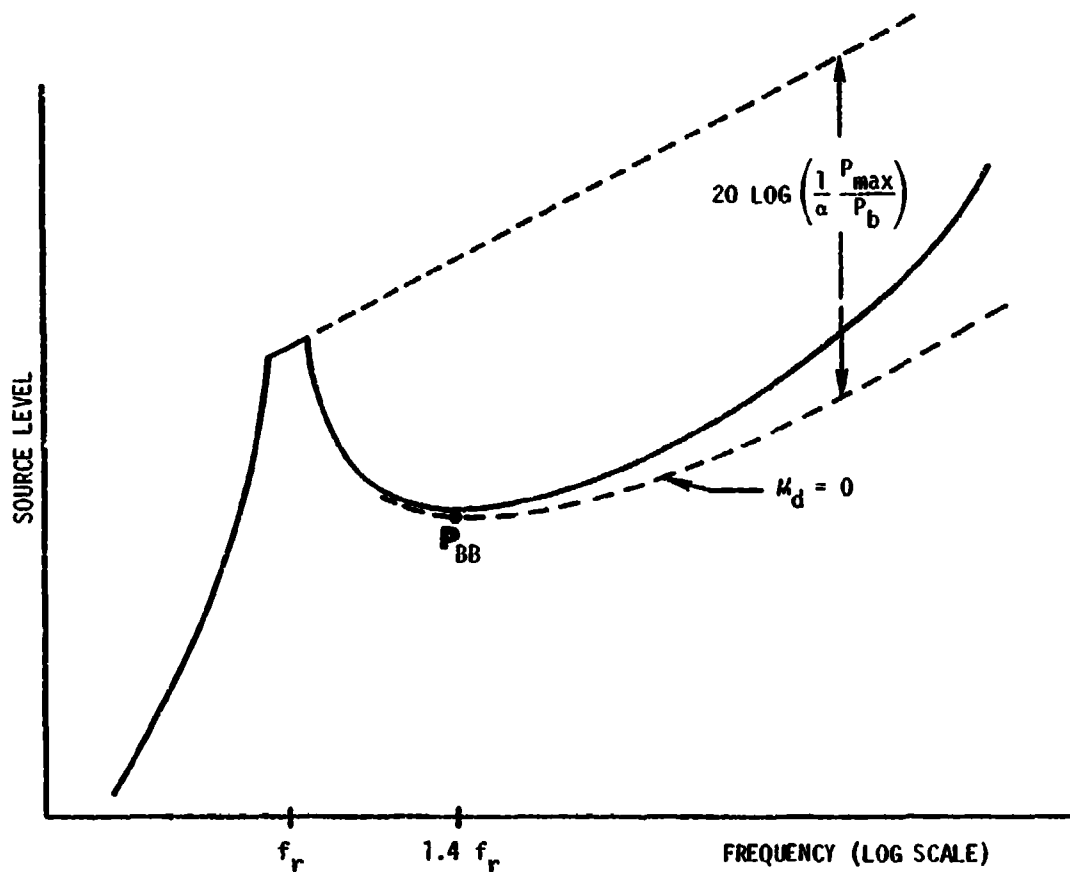


Figure 7. Maximum Source-Level Envelope. The Broadband Power P_{BB} Is Determined by the Level of the Curve at the Saddle, at a Frequency of About $1.4 f_r$

The dependence of the cavity pressure on C_c is evident from inspection of the right-hand portion of the circuit in figure 5. For a given power output (given volume velocity through R_r), a rise in cavity pressure, P , will occur when C_c is decreased; that is, when the impedance level of the parallel resonant circuit is raised. But C_c must be kept large enough so that the cavity pressure remains safely below the ceramic fracture pressure, P_{max} . Internal cavitation also limits the allowable cavity pressure. In a shallow-depth transducer, this limit may be reached before the fracture limit, in which case the choice of C_c would be based on keeping P below the cavitation level.

When both the voltage limit and the stress limit are taken into account, the result is a maximum source-level envelope, as shown in figure 7. Any desired response curve can be synthesized, by means of shaping filters or feedback networks, as long as it remains within the confines of this envelope. Figure 8 shows such a shaped source-level curve for narrowband operation, and figure 9 shows a shaped source-level curve for broadband operation. It is assumed that a more than adequate resonance rise is available to fill out the chosen envelope, which requires that both R_1 and R_2 be sufficiently low. It is preferable to omit damping in computing the source-level envelope, but to include it when computing the shaped-response curves. Figure 10 indicates circuitry that could be used to achieve maximum control over the response shape.

In the narrowband case, good efficiency becomes a possibility and hence is normally desired. Note that the term "good efficiency" is relative. Even a few percent efficiency may be considered good in a transducer whose dimensions are less than 1/50 of a wavelength. With careful attention devoted to minimizing losses, resonator Q's of the order of 100 may be achieved in favorable circumstances. While the high Q's are important for efficiency, they tend to make the bandwidth too narrow. This would be true even for single-frequency operation, since slight drifting of the resonance frequency (due, for instance, to temperature change) must be expected. This problem can be overcome by use of acoustoelectrical feedback.

The fed-back signal is derived from a hydrophone that may be either inside the compliance cavity or mounted on the outside of the transducer structure. The phase of the hydrophone signal is adjusted for negative feedback at resonance, and the signal is then mixed with the input to the driving amplifier, as shown in figure 10. The negative feedback effectively damps the resonance but does not add any real losses and hence does not affect the efficiency. In figure 8, the effective Q has been brought down to about 15 by the acoustoelectrical feedback, and the transducer has been designed so that the resulting response curve fills out the maximum source-level envelope to good advantage.

Suppose that the response peak is still considered to be too sharp, even with the Q reduced to 15. The negative feedback could be increased to reduce the effective Q further, say to 10. This would give a flatter peak, but would also lower the level of the peak. The driving voltage could then be increased to bring the response at resonance again up to the stress-limit line, and about 5 percent bandwidth would be available inside the maximum source-level envelope. All of the response curve except for this 5 percent portion would lie outside of the maximum source-level envelope, because of the raised voltage. Hence, to protect the transducer from overvoltage, the signal frequency would have to be confined carefully to the 5 percent passband region. This required control over the signal should be feasible in a narrowband system.

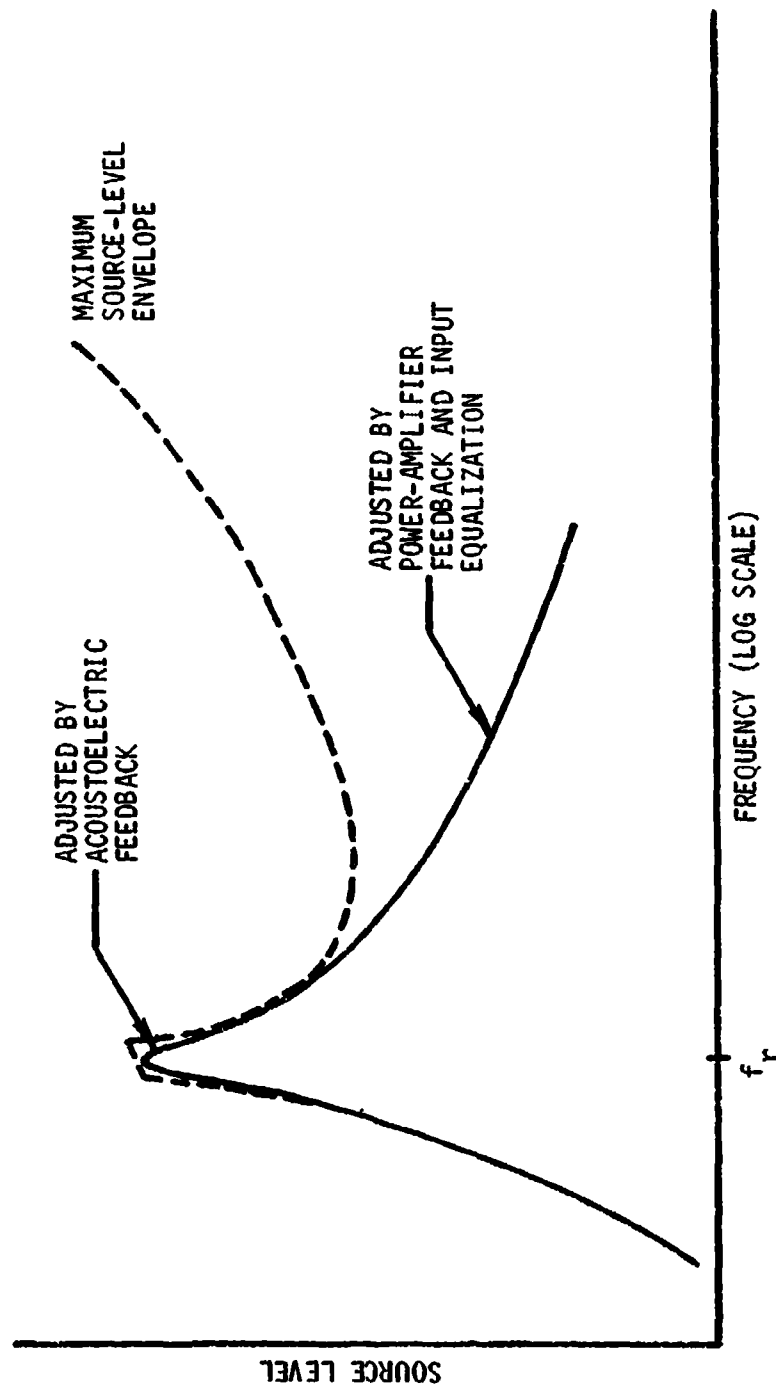


Figure 8. Shaping of the Source-Level Curve for Narrowband Applications

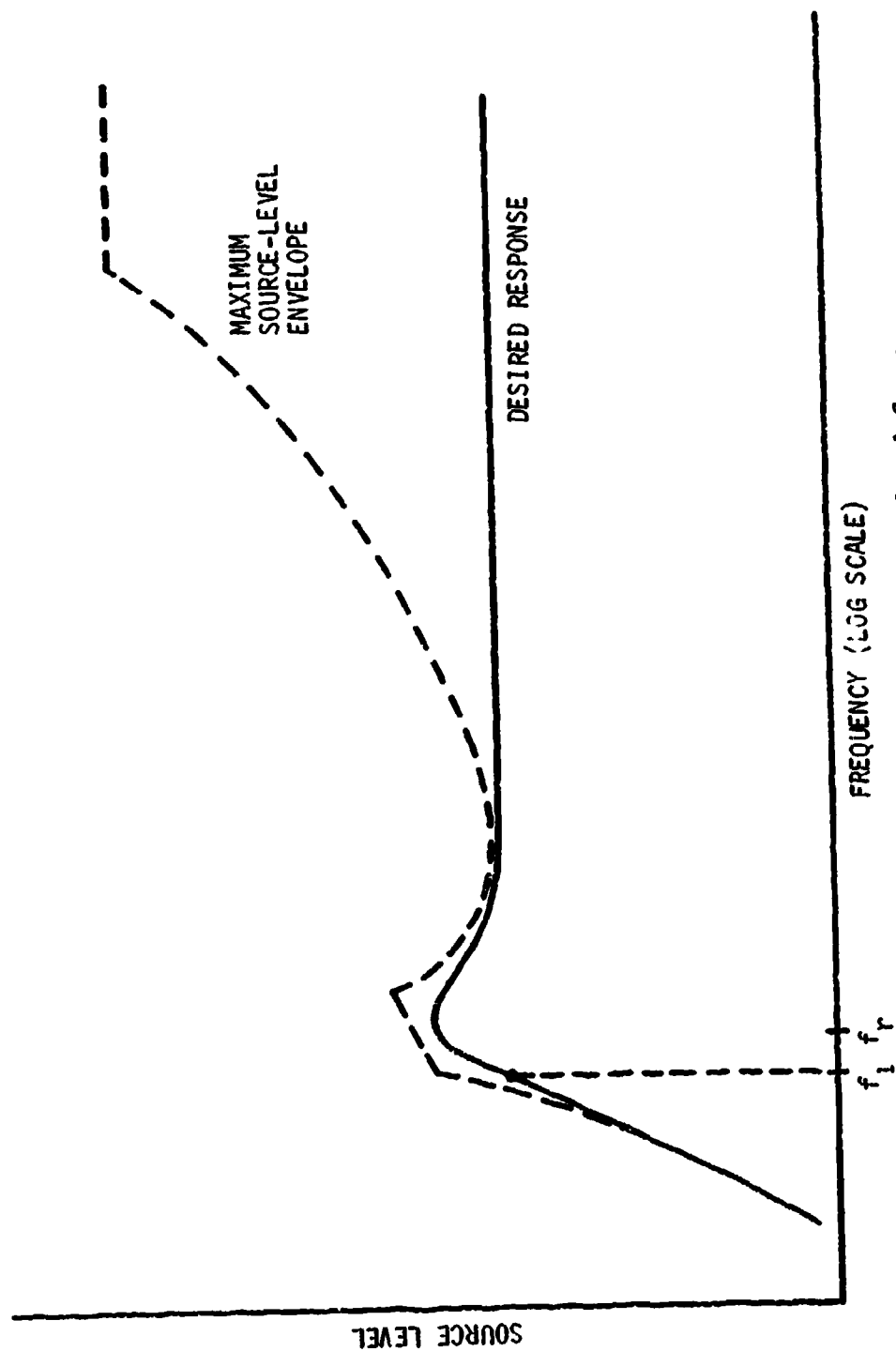


Figure 9. Shaping of the Source-Level Curve for Broadband Applications

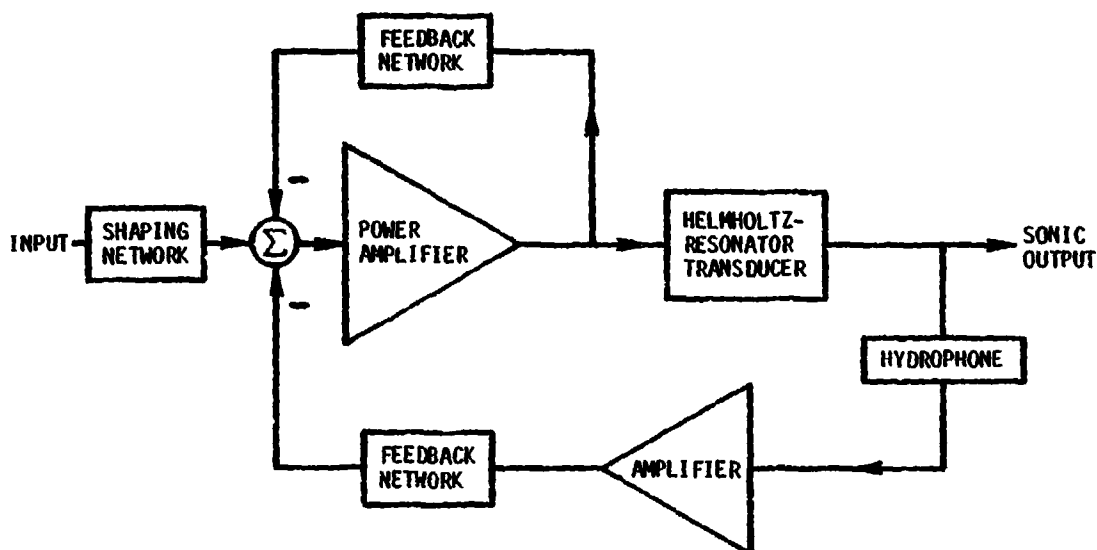


Figure 10. Circuitry for Shaping the Source-Level Curve

For intermediate bandwidth, say 20 percent, the procedure would be similar. One would lower the effective Q with feedback to around 4, and in this case the transducer would be designed to have a lower stress-limit line, since a high narrow top in the source-level envelope could not be utilized.

The rising response above resonance, shown in figure 4, is a potential source of trouble. If the signal from the power amplifier contains any harmonics, or other high-frequency distortion products, they will be greatly emphasized in the transducer output because of this rising response. If the acoustoelectrical feedback could be used to pull down this rising response, in addition to accomplishing its primary function of damping the Helmholtz resonance, this would be desirable. However, the phase margin required for stability cannot be maintained over this rising response region, so this acoustic feedback approach fails. Instead, one could add a feedback loop just over the power amplifier, as shown in figure 10. This would be used to produce a rapid fall-off in the power amplifier's response, which would overcome the rising response of the transducer. The expectation is that the negative feedback in this loop would suppress amplifier distortion to the point where it would no longer be a problem.

The remaining network, shown in figure 10 to the left of the summing point, would be used for final tailoring of the system's response. Since it is outside the feedback loops, its phase shift causes no problems and hence the network could be designed for a rather elaborate shaping function.

In the broadband case, depicted in figure 9, the effective Q can be low (e.g., 4) without destroying the benefits of resonance. These benefits include a boost in the source level at the low end (f_1) of about 12 dB over the source level that the ceramic driver could produce if the Helmholtz neck were plugged. An alternate way of describing the benefit of the resonance is to say that the low-frequency response is extended about an octave. Since the resonance rise is low, the stress-limit line can be set quite low, and this means that the cavity compliance, C_c , can be low. The crucial problem in the design is to obtain the required output at the lower cutoff frequency, f_1 . The requirements at this frequency determine the size of the ceramic driver.

The effective Q of the resonance can be brought down by acousto-electrical feedback as in the narrowband case. However, since the efficiency over the broadband is bound to be low, little would be lost by allowing high dissipative damping of the resonance, and the feedback approach might not be needed. Flattening of the response above resonance could best be done by introducing a 12 dB/octave falloff in the output of the power amplifier, by means of its local feedback loop.

CERAMIC DRIVER CHARACTERISTICS

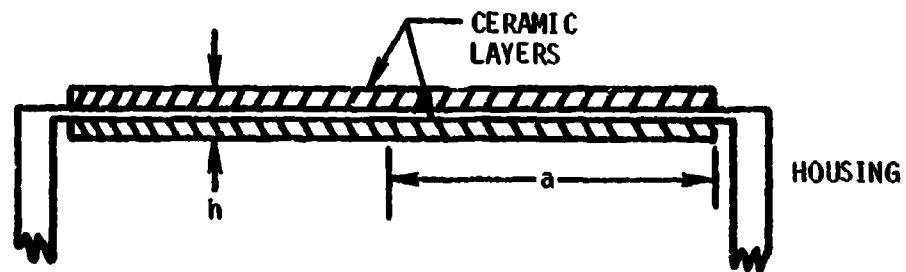
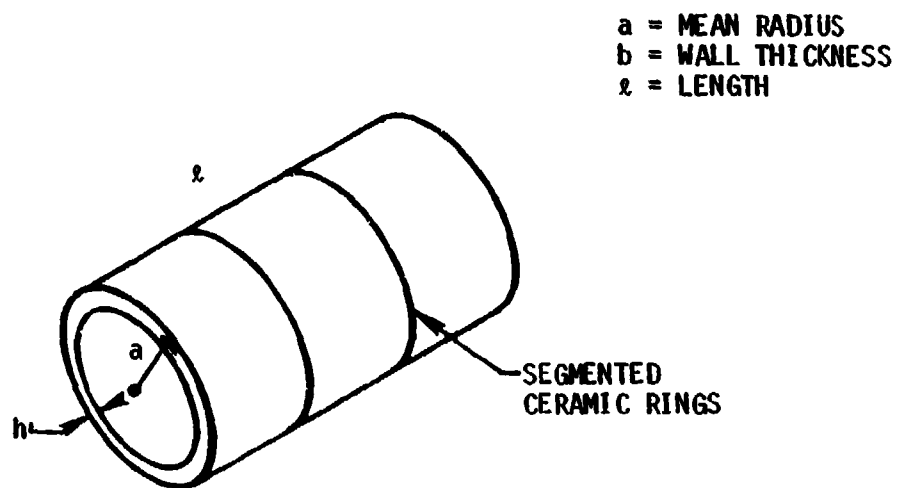
The two types of drivers under consideration are shown in figure 11. They are the stack of segmented ceramic rings, and the trilaminar flexural disk. The capabilities of the rings are simpler to describe than those of the disk. However, the disk is usually more advantageous in meeting typical design objectives. PXT-4 ceramic will be used in both drivers.

RING STACK

The free volume displacement is

$$\Delta V_f = 1.81 \times 10^{-9} a^2 l E_3, \quad (7)$$

where $E_3 = 4 \times 10^5$ V/m.



a = DISK RADIUS
 h = TOTAL THICKNESS

Figure 11. Piezoelectric Ceramic Drivers

The maximum cavity pressure is

$$P_{\max} = \frac{b}{a} T_{\max} , \quad (8)$$

where the ceramic stress limit $T_{\max} = 2000$ psi (1.4×10^7 Pa).

Other parameters of interest are the acoustical compliance,

$$C_d = 9.73 \times 10^{-11} \frac{a^2 l}{b} , \quad (9)$$

and the ratio of fracture pressure to blocked pressure,

$$P_{\max}/P_b = 1.31 , \quad (10)$$

which is fixed by the chosen values of E_3 and T_{\max} given above.

The free-volume displacement, and thus the power, depends only on the envelope volume, $\pi a^2 l$, of the ring stack, not on its aspect ratio, l/a , or wall thickness, b . The fracture pressure, P_{\max} , is determined by the wall thickness; thus it may be specified independently of ΔV_f . However, it is not practical to choose the wall thickness solely on the basis of the desired P_{\max} . To avoid unacceptable fragility it is probably necessary that $\frac{b}{a} > 1/10$; then $P_{\max} > 1.4$ MPa.

To make full use of the high-strength capability of the rings would require:

1. Deep operation (at least 140 m) to avoid cavitation at an acoustic pressure equal to P_{\max} ;
2. Operation high on the resonance curve, which means narrow bandwidth; and
3. Small cavity compliance, C_c , which has some undesirable effects, as listed in General Design Principles.

A minor inconvenience sometimes encountered is that the volume required for C_c may be less than the available volume inside the ring stack, which is approximately $\pi a^2 l$. In such a case, the volume of the transducer is not used to best advantage.

The technology for making large segmented-ceramic rings is well developed. Rings up to 2 meters in diameter have been constructed in the past.¹²

TRILAMINAR DISK

If the three layers of the disk are of equal thickness (a common condition), the free-volume displacement is

$$\Delta V_f = 1.94 \times 10^{-10} \left(\frac{a}{h} \right)^3 E_3, \quad (11)$$

where $E_3 = 4 \times 10^5$ V/m.

The maximum cavity pressure is

$$P_{\max} = 0.81 \left(\frac{h}{a} \right)^2 T_{\max}, \quad (12)$$

with $T_{\max} = 2000$ psi (1.4×10^7 Pa).

The acoustical compliance is

$$C_d = 1.38 \times 10^{-11} \left(\frac{a}{h} \right)^3 a^3. \quad (13)$$

The chosen values of E_3 and T_{\max} determine the ratio

$$P_{\max}/P_b = 1.40. \quad (14)$$

The two parameters ΔV_f and P_{\max} are no longer independent as they were for the ring; both depend on the thickness-to-radius ratio, h/a . For constant h/a , the output power goes up as the 6th power of the disk diameter, as may be seen from equations (5) and (11). Hence, primary emphasis is always on using as large a disk as possible. Equation (11) also shows that the power is proportional to $\left(\frac{h}{a} \right)^{-2}$. In other words, the thinner the disk the more volume displacement it will produce at maximum driving field, E_3 . However, the thin disk has low strength, as shown by equation (12). Therefore, a compromise must be struck between the conflicting requirements of ΔV_f and P_{\max} .

The practical range for the thickness-to-radius ratio is judged to cover

from $h/a = 0.05$, with $P_{\max} = 0.028$ MPa (4.1 psi),

to $h/a = 0.3$, with $P_{\max} = 1.02$ MPa (145 psi)

The largest trilaminar disks built to date have been under 0.5 m in diameter. However, there is no technological barrier limiting them to that size. In looking for a practical size limit, one may start with the limitation that the ceramic plates used (in the manner of tiles) to construct the ceramic layers of the trilaminar disk are available in thicknesses only up to 2 cm. This is a basic limitation of the ceramic art to date. Pieces of greater thickness cannot be effectively poled. Also, thicker ceramic might lead to problems with high voltage; even with 2 cm plates the maximum transducer voltage will have reached 8000 Vrms. The ceramic layers must constitute a sizeable fraction of the total thickness, h . Therefore, with 4 cm of the thickness devoted to ceramic, a maximum value of h of about 12 cm might be appropriate. Then if h/a were chosen to be 0.15, the disk diameter would be 1.6 m. Such a disk seems technologically feasible, but cost experience is lacking.

Since limits on disk diameter can be foreseen, the possibility of using a number of disk drivers in a single Helmholtz resonator should be considered. Practical configurations appear to be limited to two disks. Such a double-disk Helmholtz resonator is sketched in figure 12. A number of radial necks are used, and they have been placed

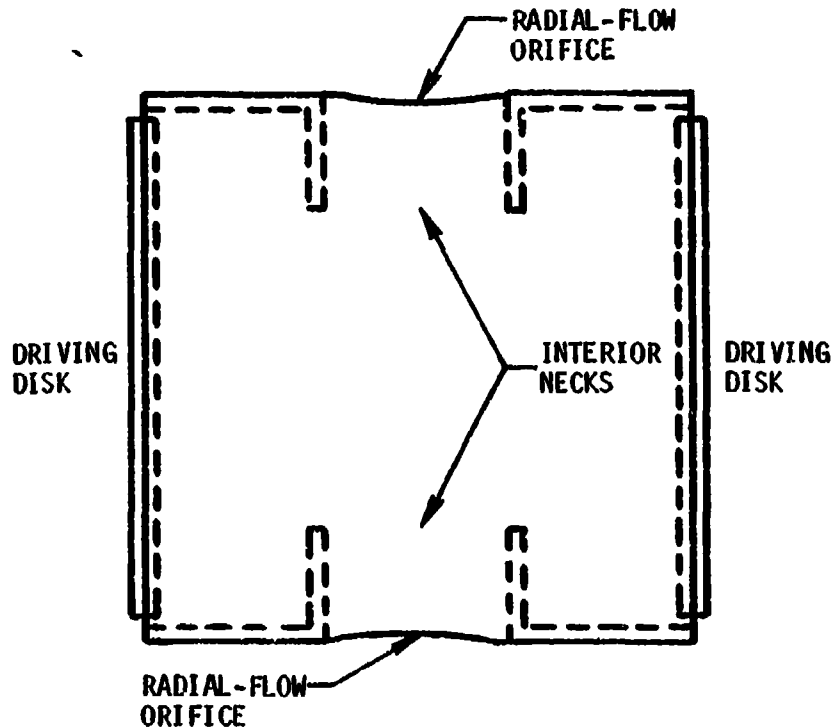


Figure 12. Double-Disk Helmholtz Resonator
With Radial-Flow Ports

inside the cavity in order to keep down the overall diameter of the transducer. Doubling the number of disks will give twice the volume displacement, or four times the power. The double-disk transducer is equivalent to a single-disk transducer whose diameter is $2^{1/3}$, or 1.26 times, greater.

COMPARISON OF RING WITH DISK

Since the primary function of the driver is to produce volume displacement, the ring and disk capabilities should be compared on that basis. The discussion above shows that disk drivers appear to best advantage in large-diameter squat resonators. The performance of ring drivers, on the other hand, is indifferent to resonator shape. If the resonator were constrained by available space to be a long small-diameter cylinder, the ring driver would probably be preferable.

When there are no constraints on resonator shape, a meaningful comparison can be obtained by letting each driver have the same radiating area and the same diameter (2a). From equations (7) and (11), it can be determined that if $h/a < 0.21$ (thin disks) the disk will have the greater volume displacement, but if $h/a > 0.21$ the ring stack will have the greater volume displacement. Thus, when the design calls for use of a thick disk, consideration should be given to using rings instead. But thick disks or rings will be called for only if the resonator is designed for high ac cavity pressure. For the disk with $h/a = 0.21$, $P_{\max} = 0.50$ MPa. If the ring driver is used instead, P_{\max} will jump to about 1.4 MPa. Such high cavity pressures are usually not desired because of the large operating depths required to suppress cavitation. Hence thin large-diameter disks are usually the preferred drivers.

NARROWBAND DESIGN

The desired source-level envelope (figure 7) for this case will have 5 percent bandwidth at the top of the truncated resonance curve. This condition is imposed because it is believed that trying to work with bandwidths less than 5 percent would be unwise, since slight drift in the resonance frequency is to be expected. Specifying this feature of the source-level envelope determines a value for the compliance ratio, α , if the type of driver also has been specified (determining P_{\max}/P_b). For a disk driver and the 5 percent envelope top, $\alpha = 0.072$. This value appears satisfactory. The factor $(1 - \alpha)^2$ in equation (5) will be 0.86, indicating close to ideal power capacity. The electro-acoustical coupling factor will be low but not disastrously so. It is given by the equation

$$k = \sqrt{\alpha} k_d \approx 0.1, \quad (15)$$

where k_d is the electromechanical coupling factor of the disk operating alone.

The remaining design considerations will be dominated by the desire to obtain good efficiency over the narrow band. The electroacoustical circuit in figure 5 shows three dissipative elements: G_b , R_d , and R_l . In addition there are the nonlinear losses associated with high-velocity flow through the resonator neck. The conductance G_b represents dielectric loss in the ceramic, and it cannot be reduced, but its effect on the efficiency is low if the coupling factor k is reasonably high. The resistance R_d , which is associated with the driver, represents losses in the potting compound or other waterproofing materials that may be used. Minimization of these losses is done by borrowing current art from other transducer developments.

The viscous loss in the cavity, represented by R_l , is a major contributor to low efficiency, so its minimization has to be considered carefully. The relation between R_l and the Q of the cavity, Q_l , is

$$R_l = \frac{1}{(1 - \alpha)\omega_r C_c Q_l}. \quad (16)$$

Obviously a high Q_l is desired, but equation (16) shows that R_l also can be reduced by making the cavity compliance C_c large. For high Q_l (low-loss cavity), one should use a liquid of low viscosity, make sure that it is well degassed, and keep the packing factor (of compliant tubes) low. Once the packing factor and liquid have been chosen, Q_l at a given frequency is assumed to become independent of cavity volume (an intensive parameter). When the next step in reducing R_l , namely increasing the cavity volume to increase C_c , is undertaken, Q_l remains constant in equation (16).

Water is satisfactory as the cavity liquid and has been used in the models to date. Its corrosive tendency is a disadvantage; so, other liquids of equally low kinematic viscosity (about $10^{-6} \text{ m}^2/\text{s}$, or 1 centistoke) will be tried. No mathematical method for calculating Q_l for a given liquid and tube pack has been found; so, this information is being obtained by experiment. Measurement of the resonator Q does not give Q_l directly, as the result contains a contribution from R_d as well as from R_l . The present methods for separating these losses are crude but hopefully will be improved. In designing for respectable efficiency, one starts with a reasonably low packing factor (e.g. 20 percent). Then, using the empirically determined Q_l for that packing

factor, the value of C_c required to meet the efficiency objective can be calculated from equation (16). This result, in turn, determines the cavity volume.

The cavity compliance called for by this procedure usually turns out to be relatively large. This implies that the ac cavity pressure will be low, and that ring drivers cannot be used advantageously. The remaining design discussion will be predicated on the use of a disk driver. Because P_{\max} and ΔV_f are not independent for the disk, design changes to increase the efficiency also will affect the power capability. Specifically, if C_c is increased to reduce R_d , the ac cavity pressure will go down. Then the disk should be made thinner (lower h/a) in order to maintain an optimum 5 percent bandwidth design (maintain $\alpha = 0.072$). A thinner disk has increased ΔV_f , so the power will go up. Everything is now better except that the cavity is larger, and its size may well be the controlling constraint. In following this procedure one may encounter the practical lower limit on thickness ($h/a \approx 0.05$). Any further increases in C_c would have to be made without the accompanying disk optimization (i.e., P_{\max} would remain larger than necessary). Another limit on increasing C_c comes about because a lower M_d is required to maintain resonance, and M_d cannot be made indefinitely small. Even after the neck length has been reduced to zero, substantial inertance remains, associated with the orifice alone.

As C_c is increased to reduce R_d , the deleterious effect of the potting resistance R_d on efficiency will increase, and this sets still another limit on how far the increase in C_c should be carried. An optimization procedure, taking all the factors that have been described into account, readily can be accomplished on the calculator mathematical model. The basic problem is not computational, but rather the physical problem of finding valid mathematical expressions, empirical or otherwise, for R_d and R_l which give their dependence on frequency, material properties, and relevant geometries.

In addition to controlling the losses in R_d and R_l , the designer must control the nonlinear losses originating in the neck. Besides its adverse effect on efficiency, the nonlinearity will cause distortion and a tendency towards saturation (nonproportional response) in the output. The latter two effects presumably could be alleviated by acoustoelectric feedback, if the feedback hydrophone is mounted outside the cavity. However, the distortion is small even without this remedy.

A semiempirical formula for neck resistance is available.¹³ It can be expressed as

$$R_{NL} = \frac{6\rho}{\omega r n} \sqrt{P}, \quad (17)$$

where

P is the output power,

ρ is the liquid density,

ω_r is the angular resonance frequency, and

A_n is the cross-sectional area of the neck.

In the circuit of figure 5 this resistance is inserted in series with M_k . The numerical factor in this equation is subject to adjustment as experience is gained. It is expected that the factor will be relatable to such neck properties as aspect ratio and corner sharpness.

Clearly a wide neck (large A_m) is needed to keep R_{NL} low. However, as the neck is made wider, it must also be made longer to maintain the inertance M_k at the value required for resonance. Once more the conclusion is reached that low loss requires large size (though the neck is not as space-consuming as the cavity). A high cavity compliance, C_c , which is desirable for high efficiency as discussed earlier, also helps here. As C_c is increased, a lower M_k will be required for resonance and a shorter neck will suffice. Multiple necks, such as indicated in figure 12, do not change the situation as far as nonlinearities go. The net resistance, R_{NL} , for a set of necks acoustically in parallel is the same as for a single neck with the same net inertance, the same total area, and the same total power flow.

BROADBAND DESIGN

When multi-octave bandwidth is required, as illustrated in figure 9, the Q of the resonance can be low (e.g., 4), and little benefit would accrue from having good efficiency at resonance. Hence, the procedures described in the previous section for minimizing losses are not of prime importance here.

The electrical input to the transducer over the broadband is mainly reactive power, and the required size and rating of the driving amplifier is determined by this reactive power rather than by the real power. Only near resonance can the real power be comparable to the reactive power; hence maximizing efficiency, which minimizes real power, is of little benefit when the band as a whole is considered. A figure of merit to replace efficiency in the broadband case is the ratio of output power (real) to reactive input power.

In forming an expression for this ratio, the approximation will be made that the electrical reactance is simply that of the free capacitance, C_f . This approximation is good, except at resonance, and even there is not bad when the resonance is highly damped. The reactive power is then $\frac{1}{2}\omega C_f E^2$, where E is the ac driving voltage, and the objective is to maximize

$$\frac{P}{\frac{1}{2}\omega C_f E^2}, \quad \text{or} \quad \omega^3(1 - \alpha)^2 \frac{(\Delta V_f)^2}{C_f E^2}.$$

For simplicity, the compliance ratio is considered to be chosen (with $\alpha \ll 1$). Then, at any given frequency the problem is to maximize

$$\frac{(\Delta V_f)^2}{C_f E^2} = k_d^2 C_d. \quad (18)$$

The coupling factor k_d is for the driver alone, and it has the approximate values of 0.4 for the disk and 0.7 for the ring.

Maximizing equation (18) calls for high driver compliance, C_d , and this means making the driver as thin as possible, whether it be a disk or a ring. However, the disk basically is capable of being much more compliant than the ring. To establish a quantitative basis for comparison of the two types of drivers, it seems best to let their volume displacements, (ΔV_f) , be equal. That is, set the right-hand side of equation (7) equal to that of equation (11). This condition imposes a geometrical relation between the two drivers, namely $a_r^2 l = 0.107 a_d^2 (a_d/h)$, where a_r is the radius of the ring and a_d is the radius of the disk. When this relation is combined with equations (9) and (13), the comparison between the disk and the ring, on the basis of equation (18), may be formulated as

$$\frac{(K_d C_d)_{\text{disk}}}{(k_d C_d)_{\text{ring}}} = 0.43 \frac{(a_d/h)^2}{(a_r/b)} \quad (19)$$

If the ring and the disk are both made as thin as practical ($b/a_r = 0.1$, $h/a_d = 0.5$), equation (19) shows that the disk is better by a factor of 17. If the disk is made thicker but the ring is kept unchanged ($b/a_r = 0.1$), the disk will lose its superiority when $h/a_d = 0.21$.

Once again the thin disk appears to be better than the ring. The limits on how thin a disk can be used are the practical limit ($h/a = 0.05$) and the need to keep α from becoming too high. High α will reduce the power, as shown by equation (5); keeping $\alpha < 0.3$ seems like a reasonable goal. To keep α low for a thin disk requires large C_c and

therefore a big compliance cavity.

The conclusions for the broadband case are similar qualitatively to those for the narrowband case. They are (1) use a disk driver rather than a ring, (2) make the disk thin, and (3) provide a large compliance cavity for best performance. Quantitatively the designs for these two cases will be different because of the difference in performance emphasis and because the limiting physical phenomena are different.

EFFECTS OF TRANSDUCER SIZE

The elementary theory of a Helmholtz resonator yields a formula for resonance frequency, $\omega_r = \sqrt{1/C_c M_\ell}$, but does not determine what the size of the resonator will be. According to this formula, the resonator could be made indefinitely small by using a small cavity (small C_c) and a very narrow neck (large M_ℓ), with the product $C_c M_\ell$ kept constant. However, as soon as the resonator is made into a transducer that must deliver significant power, size becomes all-important. As shown in the previous sections, high power requires large size, and low losses (both linear and nonlinear) do likewise. Moreover, performance (at a given frequency) improves rapidly with size.

A transducer parameter which is size-dependent and is an indicator (inverse) of potential performance is the lossless Q . With no internal losses in the transducer, this Q is determined solely by the radiation resistance. Its formula is

$$Q_0 = \frac{0.0738}{(1 - \alpha) f^3 C_c} \quad (20)$$

The lower the value of Q_0 , the better will be the expected performance. In particular, the transducer efficiency will be less sensitive to internal loss when Q_0 is low. To put this statement into quantitative form an acoustic efficiency, η_a , may be defined:

$$\eta_a = \frac{R_r}{R_\ell + R_r} = \frac{Q_\ell}{Q_\ell + Q_0} \quad (21)$$

which shows the benefits of low Q_0 . While η_a is but one factor in the overall efficiency, it is often the most important factor.

Equation (20) shows that high C_c is required to achieve low Q_0 . Normally, high C_c implies large volume; a large-volume transducer would

have a large ceramic driver (high ΔV_f) and hence high power. Thus low Q_0 is usually associated with transducers that are relatively large in terms of wavelength and have good power capability as well as good efficiency.

When the transducer size is changed in a design study, α should be kept constant in order to keep the shape of the source-level envelope unchanged. Thus, if the driver size is increased, leading to an increase in C_d , the cavity compliance C_c must be increased proportionally with C_d , leading to an increase in cavity volume.

The quantitative relation between transducer size and power is revealed readily from consideration of the ring-driven transducer. Since the free-volume displacement ΔV_f depends on the envelope volume of the ring stack (equation (7)), and since power is proportional to $(\Delta V_f)^2$, the output power is proportional to the square of the transducer volume (on the assumption that the overall volume is mainly that of the ring stack, or is proportional to the latter volume).

For a similar examination of the disk-driven transducer, it is convenient to hold h/a constant and consider increasing the diameter $2a$. Then to keep α constant requires that the length of the cavity be made proportional to a . Both the transducer volume and ΔV_f (equation (11)) will be proportional to a^3 , and thus proportional to each other. Power, being proportional to $(\Delta V_f)^2$, will be proportional to the square of the volume. The scaling principle is thus the same as for the ring-driven transducer.

Additional assumptions that seem reasonable are: (1) transducer weight is proportional to volume; and (2) cavity compliance C_c is proportional to volume. Then the scaling laws that apply when the frequency and α are kept constant can be summarized as

$$\text{Power:} \quad P \sim (\text{volume})^2$$

$$\text{Power/weight:} \quad W/\text{kg} \sim \text{volume}$$

$$\text{Lossless-Q:} \quad Q_0 \sim 1/\text{volume}$$

An upper limit on C_c exists. As C_c is made large, M_ℓ must be made small to maintain resonance, and geometric constraints are encountered in reducing M_ℓ . The equation for M_ℓ is

$$M_\ell = \frac{1}{\pi a^2} (\rho_i \ell_i + \rho_n \ell_n + \rho_w \ell_w) \quad , \quad (22)$$

where

a_n is the radius of the neck,

l_n is the length of the neck,

l_i is the interior end correction for the neck, and

l_w is the exterior end correction.

The densities ρ_i , ρ_n , ρ_w are for the fluids in the interior cavity, neck, and exterior medium, respectively. To achieve the lowest possible M_k , l_n would be made zero, but a residual effective neck length, $l_i + l_w$, would remain. The neck diameter, $2a_n$, would be made as large as possible, but a limit would be reached when it became equal to the chamber diameter, $2a$. Use of radial-flow ports (as in figure 12), would perhaps permit M_k to be reduced by a further factor of 2. For a ringstack driver, use of ports at both ends could effect a similar reduction in M_k .

It is also instructive to consider the effects of changing the frequency of a design. As an example, let the resonance frequency be changed from 20 Hz to 60 Hz; α will be kept constant. Two possible approaches to this problem are

1. Linear scaling - dimensions proportional to wavelength. The linear size of the transducer would be decreased by a factor of 3, but the power would be reduced by a factor of 9. Q_0 would be invariant.
2. Constant size - resonance raised by decreasing the neck inductance. The power would be increased by a factor of 81. Q_0 would be reduced by a factor of 27.

The second approach clearly demonstrates the benefits obtainable by increasing the ratio of transducer dimensions to wavelength (e.g., increasing $2a/\lambda$, with $2a$ being constant in this case).

For disk-driven transducers resonant well below 100 Hz, Q_0 is typically in the range 100 to 1000. However, at frequencies approaching or exceeding 100 Hz, it may be feasible to achieve much lower values of Q_0 if the designer strives for a large dimension-to-wavelength ratio. When Q_0 falls below about 30, the design procedures described so far have to be modified. In those procedures it was assumed that the transducer Q (which is always lower than Q_0) would be so high that it would be no limitation in synthesizing a response curve to fill out the source-level envelope shown in figure 6. However, when Q_0 is low, the rise in response at resonance can no longer be set at the designer's preferred level by electroacoustical feedback, but rather is determined by the transducer Q .

In the low- Q_0 case, optimum design calls for $P = P_{\max}$ at resonance, as it did in the previous cases. The stress-limit line in figure 5 is thus set to be tangent to the peak of the resonance curve. Now, however, when the transducer dimensions are varied, the stress-limit line must be moved up and down to maintain tangency; that is, α no longer is held constant. Instead of the bandwidth being chosen arbitrarily as in the previous procedures, it now has a lower limit determined by Q . The modifications to the design procedures for this case are relatively straightforward. The efficiency is markedly improved when Q_0 is low, and in general the performance is free of many of the inferior qualities that are normally associated with true VLF transducers.

In the higher frequency designs, the self-resonance frequency of the disk tends to be relatively close to the Helmholtz-resonance frequency. The transducer then becomes categorized as a coupled-resonance system and is in fact the underwater equivalent of the bass-reflex loudspeaker. Proper exploitation of the coupled resonance possibly could lead to broad bandwidth at good efficiency.

The considerations, above, of higher frequency designs lead to the conclusion that Helmholtz-resonator transducers can have advantages at frequencies well above 100 Hz as well as at the lower frequencies. However, the emphasis in this project to date is on transducers for frequencies below 100 Hz.

EFFECTS OF DEPTH REQUIREMENTS

Compliant tubes that are designed for large depths are less compressible than those designed for shallow depths. In fact, the compressibility is roughly inversely proportional to design depth. Consequently the deep transducer will require a larger compliance cavity to realize the specified C_c .

The tendency is thus for the transducer to become larger as the depth requirement is increased. For depths of more than a thousand meters the compliant tubes would be omitted and the cavity filled with liquid only. The required cavity size would then be very large. The cavity walls would have to be made thicker in order for their stiffness to remain high relative to the stiffness of the liquid interior. Hence, very deep transducers are inevitably large and heavy.

For transducers that are to be operated at fixed depth, the cavity could be filled with pressure-equalized gas in place of the liquid and compliant tubes. The cavity would then be much smaller for the same C_c and would also have low losses. The saving in transducer size would

be partially offset by the auxiliary gas storage bottles that would be required.

DESIGN PROCEDURE FOR THE DISK-DRIVEN HELMHOLTZ RESONATOR

In this section a detailed design procedure will be presented, based on the general principles discussed above. Since the flexural disk is usually the preferred driver, its use will be assumed.

It is convenient to choose the neck inertance as one of the primary design variables because it has a strong influence on the performance that can be achieved. In most cases, minimizing the inertance leads to the highest power output. An inertance ratio, K_m , is defined as follows:

$$K_m \equiv \frac{M_\ell}{\rho_w/2a} = \frac{\text{actual inertance}}{\text{full-orifice inertance}} \quad (23)$$

Full-orifice inertance means the inertance which obtains when the length of the neck is reduced to zero and the diameter is expanded until it equals that of the compliance chamber, $2a$. The cavity liquid associated with this reference orifice is taken to be water. To evaluate this inertance from equation (22), it will be assumed that the combined end corrections are represented approximately by:

$$\ell_i + \ell_w = 0.5\pi a_n \quad (24)$$

which is slightly less than twice Rayleigh's end correction for a flanged pipe radiating from one end. Then, with $\ell_n = 0$ and $a_n = 0$, equation (22) reduces to $\rho_w/2a$, the expression used in equation (23). In designing necks to realize the actual inertance, M_ℓ , it is planned to use end corrections that are being obtained from the experimental program. In the interim, equation (24) will serve as a useful first approximation for this purpose, as well as for defining the reference inertance above.

Another ratio that will be found convenient is the compressibility ratio for the cavity, γ .

$$\gamma \equiv \frac{\text{cavity compressibility}}{\text{liquid compressibility}} = (1 - F_{pk}) + F_{pk} \left(\frac{\rho c^2}{B} \right), \quad (25)$$

with

$$\frac{\rho c^2}{B} = \frac{\text{tube compressibility}}{\text{liquid compressibility}},$$

where ρc^2 is the bulk stiffness modulus of the interior liquid, B is the effective bulk stiffness modulus of the compliant tubes, and F_{pk} is the packing factor, which is the fraction of the cavity volume occupied by the tubes.

The cavity compliance is then,

$$C_c = \frac{V_c}{\rho c^2 \gamma}, \quad (26)$$

where $V_c = \pi a^2 l_c$ is the volume of the cavity.

The design process invariably requires iteration in order to achieve a suitable compromise among all the conflicting requirements. Normally the resonance frequency, required bandwidth, and maximum operating depth are specified. In the procedure presented here, these data are taken as basic and the disk diameter is chosen as the starting point for the design. The power and weight are left open, but will be brought into line with requirements, to the extent possible, by iteration of the design.

The procedure involves the following steps:

1. Choose γ (equation 25). The depth requirement determines the tube compressibility, which is determined by the ratio $\rho c^2/B$. The packing factor should be high to keep the cavity size down, but it is limited by the need to keep the viscous losses, R_l , from becoming excessive.

2. Choose α , which is chosen to make the stress limit consistent with the desired bandwidth (see figure 7). Suitable choices are: 5 percent BW, $\alpha = 0.072$; and, broadband $\alpha = 0.20$.

3. Choose K_m . Geometrical constraints require $K_m > 1$ (unless radial-flow ports are used). For maximum power, K_m should not exceed unity by any greater margin than is required to keep the cavity length, l_c , within acceptable bounds. The cavity length is found from the following equation, which gives the ratio of cavity length to diameter:

$$\frac{l_c}{2a} = \frac{1.817 \times 10^4 (1 - \alpha)}{a^2 f^2 \gamma K_m}. \quad (27)$$

4. Compute h/a . The resonance condition determines h/a . The desired equation, which is the result of combining many of the equations given earlier, is:

$$\frac{h}{a} = \left(2.72 \times 10^{-7} a^2 f_r^2 \frac{K_m}{\alpha} \right)^{1/3} . \quad (28)$$

The required depth to avoid cavitation, found from equation (12), is $0.684 \left(1620 \left(\frac{h}{a} \right)^2 - 14.6 \right)$ meters.

5. Compute the broadband power. The broadband power, P_{BB} , is defined as the power level at the saddle in the response curve (see figure 7), which occurs at a frequency of about $1.4 f_r$. An equation for P_{BB} is obtained by combining equations (5) and (11) and substituting $f = 1.4 f_r$ for the frequency. The result for a field of 4×10^5 V/m is

$$P_{BB} = 9.18 \times 10^{-6} [f_r^2 (1 - \alpha) \frac{a}{h} a^3]^2 . \quad (29)$$

6. Compute the stress-limited power. The stress-limited power at the lower cutoff frequency, f_1 , may be found from the following equation:

$$\frac{P_1}{P_{BB}} = \frac{0.1227}{\alpha \left(\frac{\alpha}{1.403} \right) + 1^2} . \quad (30)$$

7. Compute the lossless Q . Modifications of equation (20) yield the desired form for computation:

$$Q_0 = \frac{2120 K_m}{2\alpha f_r (1 - \alpha)^2} . \quad (31)$$

If $Q_0 < 30$, the resonance may be so heavily damped that the stress-limited power predicted by equation (30) will not be reached. In that event, accurate results for a narrowband design will require use of the calculator mathematical model.

8. Compute the ratio of disk resonance to operating resonance. The ratio of the two uncoupled resonances is given by the equation

$$\frac{f_{rd}}{f_r} = 1.02 \sqrt{\frac{K_m}{(1 + 6.8 h/a)(1 - \alpha)\alpha}} . \quad (32)$$

If $f_{rd}/f_r < 2.5$, the equations used in the preceding steps, which are based on simple theory that neglects the disk inertance M_d , will be of doubtful accuracy. The calculator mathematical model should then be relied on for final results.

9. Estimate orifice nonlinearity. A modification of equation (17) yields an expression for the Q that would result if there were no losses in the system except the nonlinear orifice losses. This equation is

$$Q_{NL} = \frac{20.5 f_r^2 \ell_e a^2}{\sqrt{P_r}}, \quad (33)$$

where P_r is the power output in the resonance region, and ℓ_e is the effective neck length including end corrections. Q_{NL} should be judged in relation to the overall Q_M that is required to produce the desired response rise at resonance. If Q_{NL} is higher than this desired operating Q_M , the nonlinear effects should be tolerable.

10. Estimate the transducer weight. Computation of the transducer weight is straightforward once decisions on the wall thickness of the housing structure have been made. The cavity walls are made thick enough so that their compliance is very small compared with the compliance of the interior. This is necessary, since the volume velocity due to wall motion will be out of phase with the neck-volume velocity, and therefore will diminish the radiated power. A cavity containing liquid only will require much stiffer and heavier walls than one well-packed with compliant tubes. The transducer weight is beneficial in preventing rigid-body shaking of the transducer. Some transducer motion is necessary in order to balance the momentum of the liquid in the neck, but the transducer is normally heavy enough that such motion will be small. When several radially-directed necks are used, as in figure 12, they balance each other and momentum conservation is achieved without case motion.

11. Plot response curves using the calculator mathematical model. The mathematical model consists of a calculator program for the circuit equations appropriate to figures 5 and 10, along with needed auxiliary relations, such as that giving the maximum stress in a flexural disk. It allows examination of aspects of the chosen design that are beyond the capability of the simple design equations. For example, it will show how the response can be shaped by different types of equalizers. Also, the mathematical model is basically more accurate than the simple equations, because the approximations used in the latter (principally neglect of M_d and R_d) are not used in the mathematical model.

A numerical example illustrating the procedure outlined above will now be given. The assumed specifications are: $f_r = 40$ Hz, maximum depth = 450 m, bandwidth = 5 percent. It is decided to find the performance obtainable from a flexural disk 1 m in diameter when used in a design meeting these specifications.

1. Let $\gamma = 25$. Steel compliant tubes designed for 450 m depth are available with a compliance ratio, $\rho c^2/B$, of 100 relative to water. With water used as the interior liquid, a packing factor of 25 percent should result in reasonably low damping. Equation (25) then yields $\gamma = 25$

2. Let $\alpha = 0.07$. This choice places the stress limit at a level on the resonance curve where the bandwidth is about 5 percent. The lower cutoff frequency at this level is given by the fraction $f_l/f_r = 0.976$.

3. Let $K_m = 1.69$. This makes $\ell_c/2a = 1$, or $\ell_c = 1$ m, which is considered the maximum acceptable length for the compliance chamber.

4. The ratio $h/a = 0.138$. Cavitation depth = 11 m.

5. The factor $P_{BB} = 10.7$ W, corresponding to a source level (broadband) of 183 dB/1 $\mu\text{Pa}\cdot\text{m}$.

6. The factor $P_1 = 22.7$ $P_{BB} = 380$ W, corresponding to a source level of 197 dB/1 $\mu\text{Pa}\cdot\text{m}$ over the 5 percent bandpass.

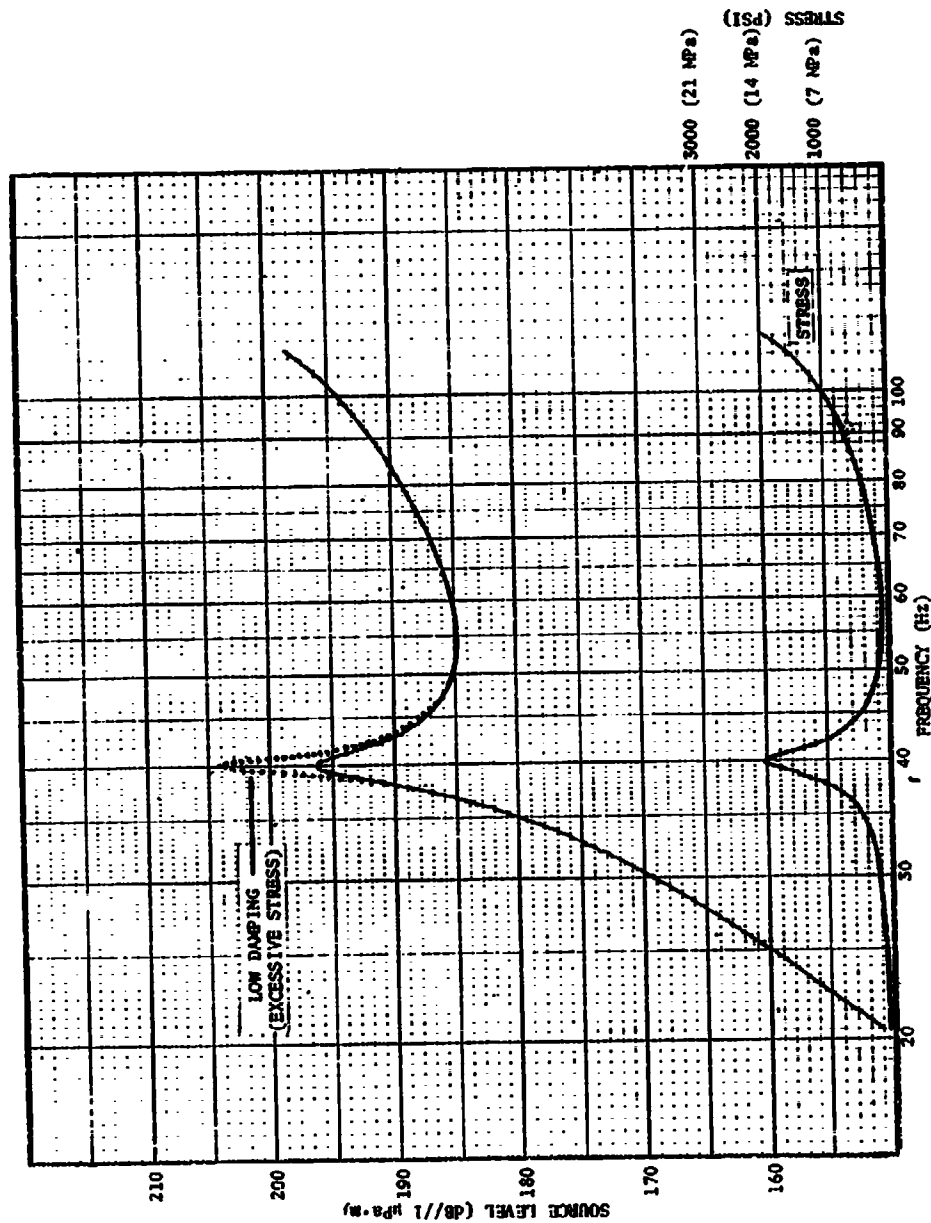
7. The factor $Q_0 = 143$.

8. The value $f_{rd}/f_r = 3.7$.

9. From equation (22) it is found that an orifice 0.6 m in diameter will provide the required inertance of 1690 kg/m⁴. $Q_{NL} = 69$, which indicates that nonlinear effects are small.

10. The wall thickness of the steel housing structure is chosen to be 2.5 cm, which makes the wall compliance about 1/50 of the interior compliance. The specific gravity of the compliant tubes is about 4. The total mass is calculated to be roughly 2500 kg. The housing structure accounts for about 28 percent of the total.

11. The source-level curve obtained by use of the calculator mathematical model is shown in figure 13. In computing the response, the voltage was maintained at its maximum value and the damping was increased until the stress was brought down to the assumed limit of 14 MPa. Although simple damping was used for convenience, equivalent results could be obtained by acoustoelectric feedback, and in that case



$h/a = 0.138$ $\alpha = 0.07$ $Q_0 = 143$ $l_c = 1$ m $2a = 1$ m $\max. \text{ depth} = 460$ m $\min. \text{ depth} = 21$ m

Figure 13. Predicted Source Level and Stress Level for a 40 Hz Helmholtz-Resonator Transducer Driven by a 1-m Disk

the efficiency would be higher than it is when the damping is deliberately made high as was done mathematically. Equalizers could be used to flatten the top of the resonance curve to fill out the region between the dotted lines at a level of 196 dB, thereby obtaining the desired 5 percent bandwidth. The mathematical model results are seen to confirm reasonably well the results obtained from the simple formulas. The source level at the saddle is about 2 dB higher than the broadband source calculated by equation (29). This shows the influence of the higher resonance (associated with M_d), which pulls up the saddle.

Several other examples of designs based on a 1-meter driving disk are given in a separate report.¹⁴ Also given are comparisons of the disks used in Helmholtz-resonator configurations with disks of the same diameter used as direct radiators.

The calculator mathematical model is capable of producing other useful results besides source-level curves such as shown in figure 13. These include efficiency as a function of frequency, equalized responses which are adjusted on the mathematical model, and integrated power of broadband random signals applied to the transducer. Examples will be given in subsequent reports.

STATUS OF HELMHOLTZ-RESONATOR INVESTIGATIONS

Model measurements have progressed far enough to generate confidence in the validity of the theory and design procedures given here. Figure 14 shows measured source-level curves¹⁵ for a model such as illustrated in figure 2, except that the packing of compliant tubes has been reduced to 16 percent for this model. The calculated curves incorporate empirical data obtained from bench measurements; that is, the damping resistances and interior distributed inertance (end correction) were derived from measurements rather than theory. For curve A, the disk was driven at full voltage in the saddle region of the response, but the drive level was rolled off at higher frequencies by a simple equalizer. Acoustoelectrical feedback from a probe hydrophone in the cavity was used to flatten the resonance, in order to demonstrate how a broadband response curve might be achieved.

Many useful data are being obtained from bench measurements, with the liquid-filled transducer in air. From the resonance frequency the interior end correction is derived, and from the Q of the resonance the damping resistances are obtained. In the studies to date (which are far from complete) Q's in the range 10 to 40 have been obtained in models employing compliant tubes. For models that are liquid filled without tubes, Q's as high as 100 have been achieved. Microbubbles increase the damping significantly and are often difficult to eliminate;

A - MAXIMUM SOURCE LEVEL, WITH RESPONSE
MODIFIED BY FEEDBACK AND EQUALIZERS
B - CONSTANT VOLTAGE RESPONSE

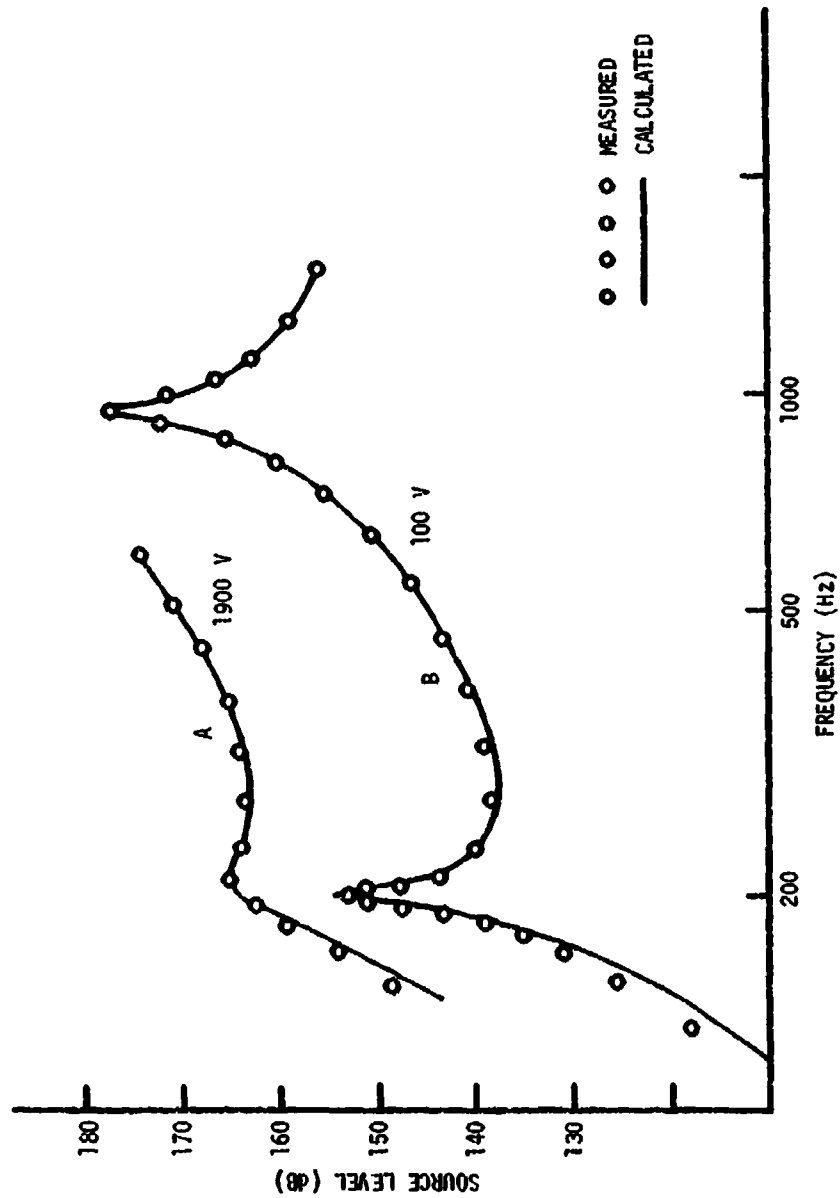


Figure 14. Measured and Calculated Source Levels for an Experimental Model

so, optimum degassing procedures are being investigated.

On the theoretical front, mathematical studies have been made, by Naval Undersea Center (NUC)¹⁶ using finite element methods, which provide a highly rigorous approach to performance calculation (except that viscosity has not yet been included).

FUTURE WORK

Much further work remains to be done with present model hardware to establish empirical rules for estimating the loss resistances of the transducer. Specifically, extensive information is required on how the cavity resistance, R_k , depends on tube size and orientation, packing factor, frequency, and viscosity. The dependence of the interior end correction on these variables is also needed, though it is of lesser importance since the neck can be adjusted to compensate for an error in the predicted end correction.

Construction of a new model is needed, to have radial-flow necks and double-disk drivers, arranged as in figure 12. The object is to verify the expected capabilities of this new approach and to get empirical data on radial-flow orificies.

Fatigue tests on metal compliant tubes are required to establish that the tubes will survive the high alternating-pressure environment of the resonator cavity.

Additional reports will be written to present the theory and computational techniques for Helmholtz-resonator transducers in greater detail.

REFERENCES

1. R. W. Dunham, "Static Compliance of Lexan Plastic Compliant Tubes from 0 to 500 psi," NUSC Technical Memorandum TD12-142-75, 23 April 1975.
2. I. D. Groves, Jr., and T. A. Henriquez, Electroacoustic Transducers for a 10,000-psig Underwater Sound Transducer Calibration Facility for the Frequency Range 10 to 4000 Hz, NRL Report 6967, 15 August 1969 (AD-693,051).
3. T. A. Henriques, The USRD Type F39A 1-kHz Underwater Helmholtz Resonator, NRL Report 7740, 10 April 1974 (AD-778,337/HH).
4. R. S. Woollett, "Very Low Frequency Broadband Transducers for Transmitting Red Noise," NUSC Technical Memorandum TD12-294-73, 5 July 1973.
5. R. S. Woollett, "Current Approaches to the Miniaturization and Pressure-Release Problems of VLF Transducers," Proceedings of the Workshop on Low-Frequency Sound Sources, NUC TP 404, September 1974 (AD/A003,894/OWH).
6. R. S. Woollett, "Piezoelectric Helmholtz Resonators," Proceedings of the Workshop on Low-Frequency Sound Sources, NUC TP 404, September 1974 (AD/A-003,894/OWH).
7. R. H. Lyon, "On the Low-Frequency Radiation Load of a Bass-Reflex Speaker," Journal of the Acoustical Society of America, vol 29, p. 654, May 1957.
8. R. S. Woollett, Theory of the Piezoelectric Flexural Disk Transducer with Applications to Underwater Sound, USL Research Report No. 490, 5 December 1960 (AD-249,731).
9. R. F. De La Croix and E. M. Cliffel, Jr., Performance Prediction Model for Radially Symmetric Flexural Disk Transducer, General Dynamics/Electro-Dynamic Div., Report No. HL 101-72, February 1972 (Contract N00140-71-C-0081).
10. E. M. Cliffel and R. F. De La Croix, Stress Computations in the General Flexural Disk Model, Hydroacoustics, Inc., Report No. HA108-73, April 1973 (Contract N00024-72-C-1295).

11. R. W. Dunham, "Control and Plotting Programs for the General Dynamics Composite Flexural Disc Analysis Routines," NUSC Technical Memorandum TD-12-208-72, 18 May 1972.
12. "Final Development Report for High-Power, Low-Frequency Transducer for RS-212," General Electric Co. (HMED), 12 June 1964.
13. G. B. Thurston, L. E. Hargrove, and B. D. Cook, "Nonlinear Properties of Circular Orifices," Journal of the Acoustical Society of America, vol. 29, pp. 992-1001, September 1957.
14. R. S. Woollett, VLF Flexural Disk Transducers Using Disks 1 Meter in Diameter, NUSC Technical Report 5509, 3 December 1976.
15. R. S. Woollett, "Underwater Helmholtz Resonator Transducers," NUSC Technical Memorandum TD12-388-75, 10 November 1975.
16. S. Spratt, "Finite Element Analysis of Low Frequency Helmholtz-Resonator Transducers," NUC TN 1614, November 1975.

INITIAL DISTRIBUTION LIST

Addressee	No. of Copies
ONR, Code 412-3	1
CNM, MAT-03, -03L	2
NRL, Underwater Sound Reference Division	2
NAVELEX, PME-124	1
NAVSEA, SEA-03C, -06H1, -06H1-2, -661T, -09G3 (4)	8
DTNSRDC	1
NAVCOASTSYS LAB	1
NAVSURFWPCEN	1
NOSC, Code 601	2
NAVPGSCOL	2
ARL/PENN STATE, STATE COLLEGE	1
DDC, ALEXANDRIA	12
ARL/U. TEXAS, AUSTIN	1
MAAG, ARGENTINA	1
MAAG, BRAZIL	1
AUWE, PORTLAND, DORSET, U.K.	1
DREA, DARTMOUTH, N.S., CANADA	1
HONEYWELL, INC, 5303 Shilshole Ave. N.W., Seattle, Washington 98107 (Mr. Leon Jones)	1
HYDROACOUSTICS INC., 321 Northland Ave., P.O. Box 3818, Rochester, N.Y. 14610 (Dr. J. V. Bouyoucos)	1
WESTINGHOUSE CORP., Baltimore-Washington International Airport, P.O. Box 1897, Baltimore, Maryland 21203 (Mr. T. B. Pederson)	1
BENDIX ELECTRODYNAMICS DIVISION, 15825 Roxford St., Sylmar, California 91342	1
INTERNATIONAL TRANSDUCER CORP., 640 McCloskey Place, Goleta, California 93017	1
MARINE RESOURCES, INC., 755 Highway 17-92, Fern Park, Florida 32730	1
MAGNAVOX CO., Fort Wayne, Indiana 46804 (Mr. E. L. Fabian)	1
RAYTHEON SUBMARINE SIGNAL DIVISION, P.O. Box 360, Portsmouth, R.I. 02871 (Mr. S. L. Ehrlich)	1
HAZELTINE CORP., Harrison Blvd., Avon, Massachusetts 02322 (Mr. Don Ricketts)	1
AEROJET ELECTROSYSTEMS CO., 1100 W. Hollyvale St., Azusa, California 91702 (Mr. Theron Lambert)	1
SPARTON ELECTRONICS, Jackson, Michigan 49202 (Mr. Alton E. Knoll)	1
AMETEK STRAZA, 790 Greenfield Dr., El Cajon, California 92022 (Mr. Glen Liddiard)	1
GENERAL ELECTRIC, Farrell Road Plant, Syracuse, N.Y. 13201	1
OCEAN & ATMOSPHERIC SCIENCE, 145 Palisade St. Dobbs Ferry, N.Y. 10522	1